Organic & Biomolecular Chemistry

Quantifying the barrier for the movement of cyclobis(paraquat-*p*-phenylene) over a monopyrrolotetrathiafulvalenium dication

Journal:	*Organic & Biomolecular Chemistry*
Manuscript ID	OB-ART-11-2021-002263.R1
Article Type:	Paper
Date Submitted by the Author:	21-Jan-2022

Complete List of Authors:	Kristensen, Rikke; University of Southern Denmark, Department of Physics, Chemistry and Pharmacy Neumann, Mathias; University of Southern Denmark, Department of Physics, Chemistry and Pharmacy Andersen, Sissel; University of Southern Denmark, Department of Physics and Chemistry Stein, Paul; University of Southern Denmark, Department of Physics, Chemistry and Pharmacy Flood, Amar; Indiana University, Chemistry Department Jeppesen, Jan; University of Southern Denmark, Department of Physics, Chemistry and Pharmacy

ARTICLE

Quantifying the barrier for the movement of cyclobis(paraquat-*p*-phenylene) over the dication of monopyrrolotetrathiafulvalene†

Received 00th January 20xx,
Accepted 00th January 20xx

DOI: 10.1039/x0xx00000x

Rikke Kristensen,‡[a] Mathias S. Neumann,‡[a] Sissel S. Andersen,[a] Paul C. Stein,[a] Amar H. Flood[b] and Jan O. Jeppesen*[a]

A bistable [2]pseudorotaxane **1**⊂CBPQT•4PF_6 and a bistable [2]rotaxane **2**•4PF_6 have been synthesised to measure the height of an electrostatic barrier produced by double molecular oxidation (0 to +2). Both systems have monopyrrolotetrathiafulvalene (MPTTF) and oxyphenylene (OP) as stations for cyclobis(paraquat-*p*-phenylene) ($CBPQT^{4+}$). They have a large stopper at one end while the second stopper in $\mathbf{2}^{4+}$ is composed of a thioethyl (SEt) group and a thiodiethyleneglycol (TDEG) substituent, whereas in **1**⊂$CBPQT^{4+}$, the SEt group has been replaced with a less bulky thiomethyl (SMe) group. This seemingly small difference in the substituents on the MPTTF unit leads to profound changes when comparing the physical properties of the two systems allowing for the first measurement of the deslipping of the $CBPQT^{4+}$ ring over an $MPTTF^{2+}$ unit in the [2]pseudorotaxane. Cyclic voltammetry and ^{1}H NMR spectroscopy was used to investigate the switching mechanism for **1**⊂CBPQT•$MPTTF^{4+}$ and **2**•$MPTTF^{4+}$, and it was found that $CBPQT^{4+}$ moves first to the OP station producing **1**⊂CBPQT•OP^{6+} and 2•OP^{6+}, respectively, upon oxidation of the MPTTF unit. The kinetics of the complexation/decomplexation process occurring in **1**⊂CBPQT•$MPTTF^{4+}$ and in **1**⊂CBPQT•OP^{6+} were studied, allowing the free energy of the transition state when $CBPQT^{4+}$ moves across a neutral MPTTF unit (17.0 kcal mol^{-1}) or a di-oxidised $MPTTF^{2+}$ unit (24.0 kcal mol^{-1}) to be determined. These results demonstrate that oxidation of the MPTTF unit to $MPTTF^{2+}$ increases the energy barrier that the $CBPQT^{4+}$ ring must overcome for decomplexation to occur with 7.0 kcal mol^{-1}.

Introduction

Since the first syntheses[1,2] of catenanes and rotaxanes were reported in the 1960s, scientists have been fascinated by these interlocked compounds. The advent of supramolecular chemistry[3-7] has paved the way to much more efficient protocols for the synthesis of catenanes and rotaxanes compared to the early low-yielding statistical and demanding covalently templated approaches.[2,8] The chemistry of the non-covalent bond has transformed these molecular systems from chemical curiosities into a flourishing field of modern research. Thus, it is now possible to prepare these kinds of ordered molecules by recognising the role that mechanical bonds[9] can play alongside covalent and non-covalent bonds.

These interlocked compounds have been used extensively and successfully to create artificial molecular machines (AMMs)[10] in an effort to mimic both biological processes (biomimetic[11]), such as the controlled molecular motion taking place in ATP-synthase[12,13] or kinesin's ability to walk along the microtubule filament,[14] and macroscopic processes (technomimetic[11]), such as pumps,[15-19] cars,[20] and elevators.[21] These designs often rely on controlling[15,22-24] the mechanisms of stimuli-driven motion, and thus motivate studies of kinetics[25-29] and the underlying energy landscapes.[30,31] We do this here by measuring the impact of double oxidation on the barrier to the motion of a mobile ring (Scheme 1).

[2]Catenanes[§1] and [2]rotaxanes,[§2] and in particular bistable [2]rotaxanes[29,33-36] based on the π-electron accepting tetracationic macrocycle cyclobis(paraquat-*p*-phenylene) ($CBPQT^{4+}$) and π-electron donating recognition units (stations) such as tetrathiafulvalene (TTF), dioxynaphthalene (DNP) or hydroquinone (HQ) have been shown to be excellent molecular switches.

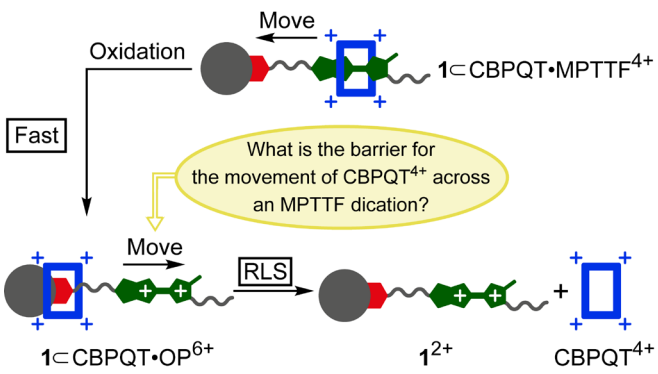

Scheme 1 Oxidation of the monopyrrolotetrathiafulvalene (MPTTF) unit in **1**⊂CBPQT•$MPTTF^{4+}$ to produce**1**⊂CBPQT•OP^{6+}, which subsequently deslips in a slow and rate-limiting step (RLS) producing $\mathbf{1}^{2+}$ and $CBPQT^{4+}$.

[a] Department of Physics, Chemistry and Pharmacy, University of Southern Denmark, Campusvej 55, DK-5230 Odense M. Denmark. E-mail: joj@sdu.dk; Tel: +45 65 50 25 87
[b] Department of Chemistry, Indiana University, 800 E. Kirkwood Avenue Bloomington, IN 47405-7102, USA

† Electronic Supplementary Information (ESI) available: ^{1}H NMR and UV-Vis-NIR spectra, binding studies and kinetic studies. See DOI: 10.1039/x0xx00000x

‡ Both authors contributed equally to this work.

The foundation for the success of switching is the TTF unit's capability to be oxidised reversibly[37-39] first to its radical cation ($TTF^{\bullet+}$) and secondly to the dication (TTF^{2+}), which creates an electrostatic repulsion between the positively charged TTF unit and the tetracationic $CBPQT^{4+}$ ring forcing $CBPQT^{4+}$ to move away from the oxidised TTF station to end up at another station (*i.e.* DNP or HQ).

In order to control the switching rate of the movement of $CBPQT^{4+}$, different barriers, either steric or electrostatic[40-45] as well as photo-switchable gates and dynamic foldameric linker regions[43,46] have been incorporated in the dumbbell component between the stations. The kinetic data emerging from these systems have provided knowledge about the movement of $CBPQT^{4+}$ away from the positively charged TTF unit ($TTF^{\bullet+}/TTF^{2+}$). Few studies, however, have been directed at examining whether the TTF^{2+} unit itself can act as an electrostatic barrier for $CBPQT^{4+}$, *i.e.* is it possible for $CBPQT^{4+}$ to cross a TTF^{2+} unit? To the best of our knowledge, only two studies have been directed toward this end. An exemplary study by Stoddart and co-workers[47] made use of atomic force microscopy (AFM) to measure the force that was needed to pull the $CBPQT^{4+}$ ring across the electrostatic barrier of a TTF^{2+} unit in a bistable [2]rotaxane attached to a silicon surface. It was concluded that that the electrostatic barrier energy for the $CBPQT^{4+}$ ring to cross the TTF^{2+} unit was 65 kcal mol^{-1}, a value that does not allow the $CBPQT^{4+}$ ring to cross TTF^{2+} under normal conditions unless it is forced to do so (by pulling with an AFM tip).[§3] However, in a recent study by some of us, it was reported that in a tetra-stable [2]rotaxane[25] incorporating $CBPQT^{4+}$ as the ring component and TTF, monopyrroloTTF (MPTTF), HQ and oxyphenylene (OP) as stations, the $CBPQT^{4+}$ ring can cross both an $MPTTF^{2+}$ and a TTF^{2+} unit under stress-free conditions (*i.e.* no pulling of $CBPQT^{4+}$ is applied) at room temperature and in a time scale of less than 20 min. It was estimated that the free energy of activation required for $CBPQT^{4+}$ to move across the $MPTTF^{2+}$ unit is *ca.* 0.5 kcal mol^{-1} smaller compared to TTF^{2+}. Although it was demonstrated qualitatively that the $CBPQT^{4+}$ ring can move across both an $MPTTF^{2+}$ and a TTF^{2+} unit under relatively mild conditions, the free energy of activation ($\Delta G^{\ddagger}$) for the processes could not be determined.

In this paper, we describe the synthesis and characterisation of a bistable [2]pseudorotaxane[§4,§5,48-51] **1**⊂CBPQT•$4PF_6$ (Fig. 1) and a model [2]rotaxane **2**•$4PF_6$, and the thermodynamic and kinetic characteristics of the [2]pseudorotaxane **1**⊂CBPQT•$4PF_6$. Both **1**⊂CBPQT•$4PF_6$ and **2**•$4PF_6$ contain two potential stations for $CBPQT^{4+}$, namely a primary redox-active MPTTF station (green) and a secondary OP station (red). They are both constructed in such a way that the pyrrole moiety of the MPTTF unit point toward the OP station, which is directly connected to a conventional large triarylmethyl[§6] stopper. In the [2]rotaxane **2**•$4PF_6$, the second stopper is a smaller and more unconventional one that is composed of a thioethyl (SEt) group and a thiodiethyleneglycol (TDEG) substituent.[40] By replacing the SEt group with a less bulky thiomethyl (SMe) group, the $CBPQT^{4+}$ ring (blue) possesses enough thermal energy at room temperature to permit its slow passage over the combination of the SMe group and the TDEG substituent[25,27,52] destroying the interlocked nature of the system and therefore convert it into a [2]pseudorotaxane (*i.e.* **1**⊂CBPQT•$4PF_6$).

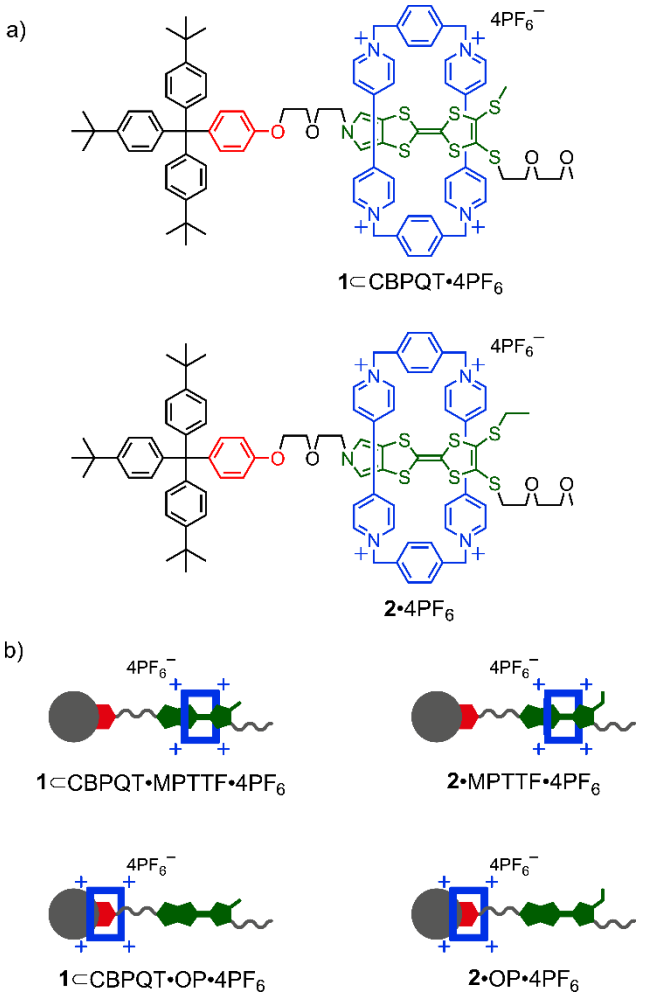

Fig. 1 a) Molecular structures of the bistable [2]pseudorotaxane **1**⊂CBPQT•$4PF_6$ and the bistable [2]rotaxane **2**•$4PF_6$ (only one translational isomer for each is shown). b) Cartoon representations of the two possible translational isomers of **1**⊂CBPQT•$4PF_6$ and **2**•$4PF_6$, respectively. It is noted that the only difference between the [2]pseudorotaxane and the [2]rotaxane is the exchange of a thiomethyl (SMe) group attached to the MPTTF unit (green) in **1**⊂CBPQT•$4PF_6$ with a thioethyl group (SEt) in **2**•$4PF_6$.

Binding studies, as well as ^1H NMR and UV-Vis-NIR spectroscopic investigations, of **1**⊂CBPQT•$4PF_6$ and **2**•$4PF_6$ showed that they exclusively exist as the translational isomers **1**⊂CBPQT•MPTTF•$4PF_6$ and **2**•MPTTF•$4PF_6$, respectively, in which the MPTTF station is located inside the $CBPQT^{4+}$ ring (Fig. 1b). The outcome is a bistable [2]pseudorotaxane and a bistable [2]rotaxane capable of switching between its two stations induced by electrochemical stimuli. During these investigations, we discovered that the switching in [2]pseudorotaxane **1**⊂$CBPQT^{4+}$ was not confined. Instead, our electrochemical and ^1H NMR spectroscopic investigations revealed that the $CBPQT^{4+}$ ring is only temporarily located at the OP station to produce **1**⊂$CBPQT•OP^{6+}$ (Scheme 1), and thereafter the $CBPQT^{4+}$ ring deslips from the oxidised semidumbbell to produce (Scheme 1) the

uncomplexed species $\mathbf{1}^{2+}$ and $CBPQT^{4+}$, respectively. This observation allowed us not only to monitor the deslipping process but also to quantify the size of the electrostatic barrier when $CBPQT^{4+}$ moves across an $MPTTF^{2+}$ unit.

Results and discussion

Synthesis

The syntheses of the large triarylmethyl stopper **3**,[33] the MPTTF derivatives **4**[53] and **5**,[40] and CBPQT•$4PF_6$[54] have already been reported. Here, we describe the synthesis of the [2]pseudorotaxane **1**⊂CBPQT•$4PF_6$ and the [2]rotaxane **2**•$4PF_6$ as outlined in Schemes 2 and 3. Deprotonation of the pyrrole *N*-H proton in the MPTTF derivatives **4** and **5** using NaH in DMF followed by *N*-alkylation of the corresponding anions with the iodide **3** carrying the large triarylmethyl stopper gave the semidumbbell **1** and the dumbbell **6** in 72 and 78% yields, respectively.

Mixing the yellow semidumbbell **1** with equimolar amounts of the colourless CBPQT•$4PF_6$ ring in Me_2CO/CH_2Cl_2 (20:1) at 298 K gave a yellow solution, which slowly became green, an observation related[55] to slow formation (Scheme 2) of the [2]pseudorotaxane **1**⊂CBPQT•$4PF_6$. Allowing the mixture to equilibrate for 16 h, followed by fast flash column chromatography, made it possible to separate the [2]pseudorotaxane

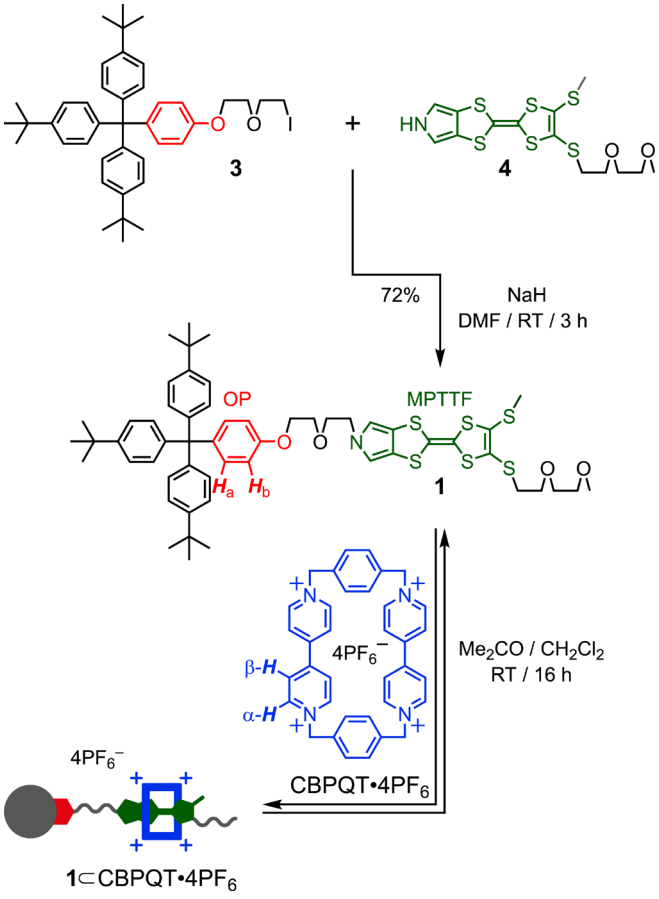

Scheme 2 Synthesis of the semidumbbell **1** and self-assembly of the [2]pseudorotaxane **1**⊂CBPQT•$4PF_6$.

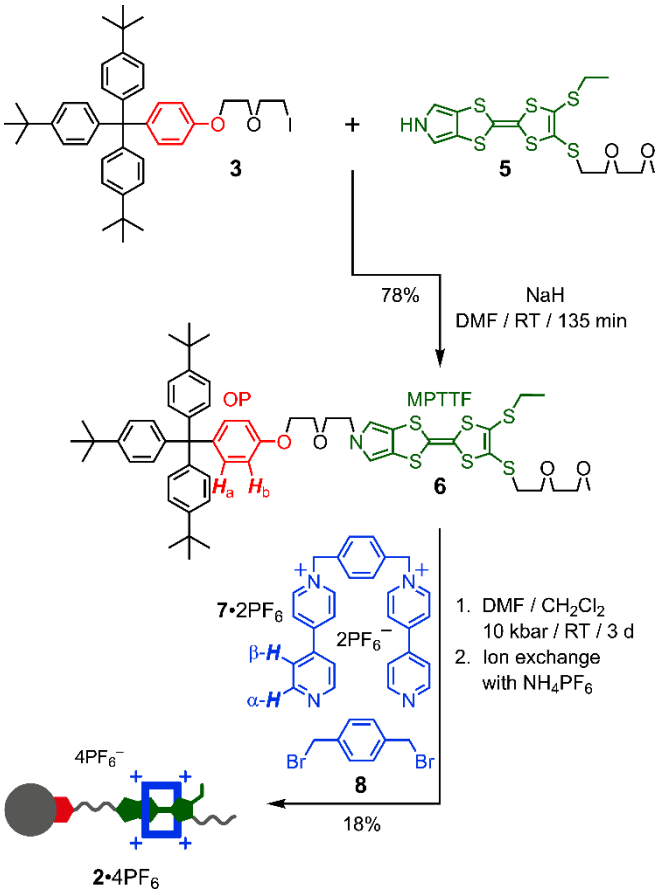

Scheme 3 Synthesis of the dumbbell **6** and the [2]rotaxane **2**•$4PF_6$.

1⊂CBPQT•$4PF_6$ from the uncomplexed semidumbbell **1** and excess CBPQT•$4PF_6$, providing the [2]pseudorotaxane **1**⊂CBPQT•$4PF_6$ as a green residue/solid, which was re-dissolved in MeCN and stored cold at 232 K.

For the synthesis of the [2]rotaxane **2**•$4PF_6$, a high pressure reaction was carried out by using the dumbbell **6** as the template for the formation (Scheme 3) of the encircling $CBPQT^{4+}$ ring. The [2]rotaxane **2**•$4PF_6$ was self-assembled by subjecting a mixture of the dumbbell **6**, 1′′-[1,4-phenylenebis(methylene)]bis(4,4′-bipyridinium) bis(hexafluorophosphate)[54] (**7**•$2PF_6$) and 1,4-bis(bromomethyl)benzene (**8**) in DMF/CH_2Cl_2 (11:1) to ultra-high pressure (10 kbar) for 3 d followed by counterion exchange affording **2**•$4PF_6$ as a green solid in 18% yield.

Photophysical investigations

The photophysical properties of the semidumbbell **1**, $CBPQT^{4+}$, the [2]pseudorotaxane **1**⊂$CBPQT^{4+}$, the dumbbell **6** and the [2]rotaxane $\mathbf{2}^{4+}$ were investigated in MeCN at 298 K. The UV-Vis-NIR absorption spectra of $CBPQT^{4+}$ (Fig. 2a) did not display any absorption bands in the visible spectral region and the solution appears colourless. The semidumbbell **1** (Fig. 2a) and the dumbbell **6** (Fig. 2b) only exhibit weak tails in the visible region at $\lambda \leq 500$ nm and these solutions, thus, appear yellow.

Mixing equimolar proportions of the semidumbbell **1** and $CBPQT^{4+}$ in MeCN initially produced a yellow solution, which

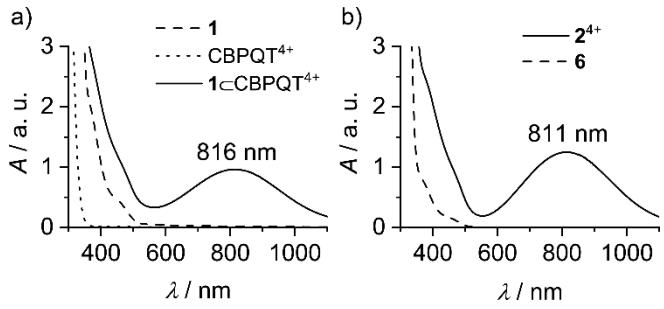

Fig. 2 UV-Vis-NIR absorption spectra recorded in MeCN at 298 K of a) the semidumbbell **1** (0.8 mM), $CBPQT^{4+}$ (0.8 mM) and an equilibrated 1:1 mixture of **1** and $CBPQT^{4+}$ (0.8 mM) and b) the dumbbell **6** (0.3 mM) and the [2]rotaxane $\mathbf{2}^{4+}$ (0.8 mM).

upon standing slowly became green. This colour change was accompanied by the appearance of a charge-transfer (CT) band centered on 816 nm in the UV-Vis-NIR absorption spectrum (Fig. 2a), a situation which is characteristic[56] of a superstructure in which the MPTTF unit is located inside the cavity of $CBPQT^{4+}$. This sequence of events unambiguously reveals that the [2]pseudorotaxane **1**⊂CBPQT•$MPTTF^{4+}$ is formed upon mixing **1** and $CBPQT^{4+}$ and that the combination of the SMe group and the TDEG substituent does not constitute a stopper group for $CBPQT^{4+}$ at 298 K. After 16 h no perceptible changes were observed in the absorption spectra indicating that the equilibrium between the uncomplexed species (*i.e.* **1** and $CBPQT^{4+}$) and the [2]pseudorotaxane **1**⊂CBPQT•$MPTTF^{4+}$ was reached.

The UV-Vis-NIR absorption spectrum (Fig. 2b) recorded of a solution of the [2]rotaxane $\mathbf{2}^{4+}$ showed a broad absorption band at 811 nm and the colour of the solution appears green, indicating that the MPTTF unit is encircled by $CBPQT^{4+}$.

^{1}H NMR spectroscopic investigations

While UV-Vis-NIR spectroscopy indicates qualitatively the presence of $CBPQT^{4+}$ on the rod section of the semidumbbell and dumbbell components of the [2]pseudorotaxane **1**⊂$CBPQT^{4+}$ and [2]rotaxane $\mathbf{2}^{4+}$, respectively, ^{1}H NMR spectroscopy was used to provide more precise information about the interactions taking place between $CBPQT^{4+}$ and the semidumbbell/dumbbell.

From the ^{1}H NMR spectrum (400 MHz) recorded (Fig. S1†) of the [2]rotaxane $\mathbf{2}^{4+}$ in CD_3CN at 298 K, it is clearly evident that $CBPQT^{4+}$ is present by the appearance of an AB system (J_{AB} = 13.4 Hz) integrating for eight protons at δ = 5.69 and 5.72 ppm and three broad singlets at δ = 8.81 (4H), 8.97 (2H) and 9.05 (2H) ppm, which can be assigned to the $^+NCH_2$ protons and the α-*H* protons, respectively, located in the $CBPQT^{4+}$ ring. A comparison of the ^{1}H NMR spectra (400 MHz, 298 K) of the dumbbell **6** and the [2]rotaxane $\mathbf{2}^{4+}$ recorded in CD_3CN reveal significant chemical shift differences for the resonances associated with the protons located closest to the MPTTF unit, suggesting that the MPTTF unit is located inside the $CBPQT^{4+}$ ring in the [2]rotaxane $\mathbf{2}^{4+}$. The most diagnostic evidence, which shows that the $CBPQT^{4+}$ ring encircles the MPTTF unit, is the downfield shift of the resonance for the two methylene protons in the SEt group and the upfield shift of the resonance for the two pyrrole-*H* protons. The SCH_2CH_3 protons resonate as a quartet (J = 7.4 Hz) at δ = 3.10 ppm and the pyrrole-*H* protons[57] as an AB system (J_{AB} = 2.0 Hz) at δ = 6.22 and 6.25 ppm in the [2]rotaxane $\mathbf{2}^{4+}$ compared with a quartet (J = 7.4 Hz) at δ = 2.84 ppm (SCH_2CH_3) and a singlet at δ = 6.63 ppm (pyrrole-*H*) in the dumbbell **6**.

Because the [2]rotaxane $\mathbf{2}^{4+}$ contains two potential stations (*i.e.* MPTTF and OP) for $CBPQT^{4+}$, it can, in principle, exist as a mixture of two translational isomers. One (*i.e.* **2**•$MPTTF^{4+}$), in which $CBPQT^{4+}$ encircles the MPTTF station, and the other (*i.e.* **2**•OP^{4+}) in which $CBPQT^{4+}$ encircles the OP station. Since the [2]rotaxane $\mathbf{2}^{4+}$ is constructed in such a way that the pyrrole moiety of the MPTTF unit point toward the OP station, the shuttling of $CBPQT^{4+}$ between the MPTTF and OP stations is expected to be fast on the ^{1}H NMR timescale because the steric barrier exhibited from the planar pyrrole moiety is less than 15 kcal mol^{-1}.[58] This is supported by the fact that only one set of signals are observed in the ^{1}H NMR spectrum (400 MHz) recorded (Fig. S1†) of the [2]rotaxane $\mathbf{2}^{4+}$, which show that the exchange between the **2**•$MPTTF^{4+}$ and **2**•OP^{4+} translational isomers occurs rapidly on the ^{1}H NMR time scale (CD_3CN, 400 MHz) at 298 K. Thus, the chemical shift values of the observed resonances are weighted average values between those for the **2**•$MPTTF^{4+}$ and **2**•OP^{4+} translational isomers. Consequently, the population between the two isomers cannot be quantified from the ^{1}H NMR spectrum. However, in a [2]rotaxane containing only an MPTTF station in the dumbbell component and $CBPQT^{4+}$ as the ring component, it was observed that the SCH_2CH_3 protons resonate at δ = 3.03 ppm,[53] which is very close to the value (3.10 ppm) observed for the same protons in the [2]rotaxane $\mathbf{2}^{4+}$, strongly suggesting that the [2]rotaxane $\mathbf{2}^{4+}$ mainly exists as **2**•$MPTTF^{4+}$. This is in full agreement with the fact that the binding affinity (*vide infra*) between the MPTTF derivative **9** (Fig. 3) and $CBPQT^{4+}$ ($\Delta G°$ = –6.0 kcal mol^{-1}) is significantly larger as compared to the binding affinity between the OP derivative **10** (Fig. 3) and $CBPQT^{4+}$ ($\Delta G°$ = –1.7 kcal mol^{-1}).[27] Assuming that the relative populations between **2**•$MPTTF^{4+}$ and **2**•OP^{4+} are related to the Gibbs free energy difference ($\Delta\Delta G°$) for the binding affinity between $CBPQT^{4+}$ and the MPTTF derivative **9** and the OP derivative **10**, respectively, it can be calculated[§7] that the relative populations of **2**•$MPTTF^{4+}$ and **2**•OP^{4+} at equilibrium are 99.9% and 0.1%, respectively, in CD_3CN at 298 K.

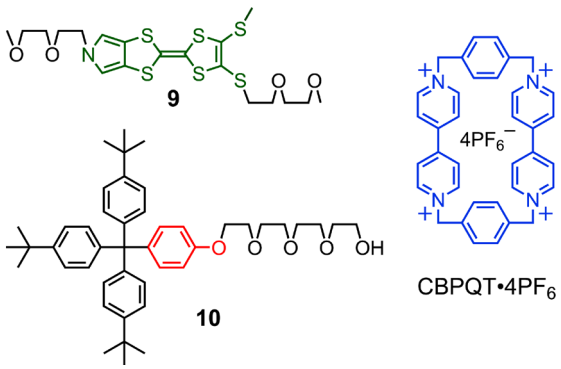

Fig. 3 Molecular formulas of the model compounds **9** and **10** and the macrocycle CBPQT•$4PF_6$.

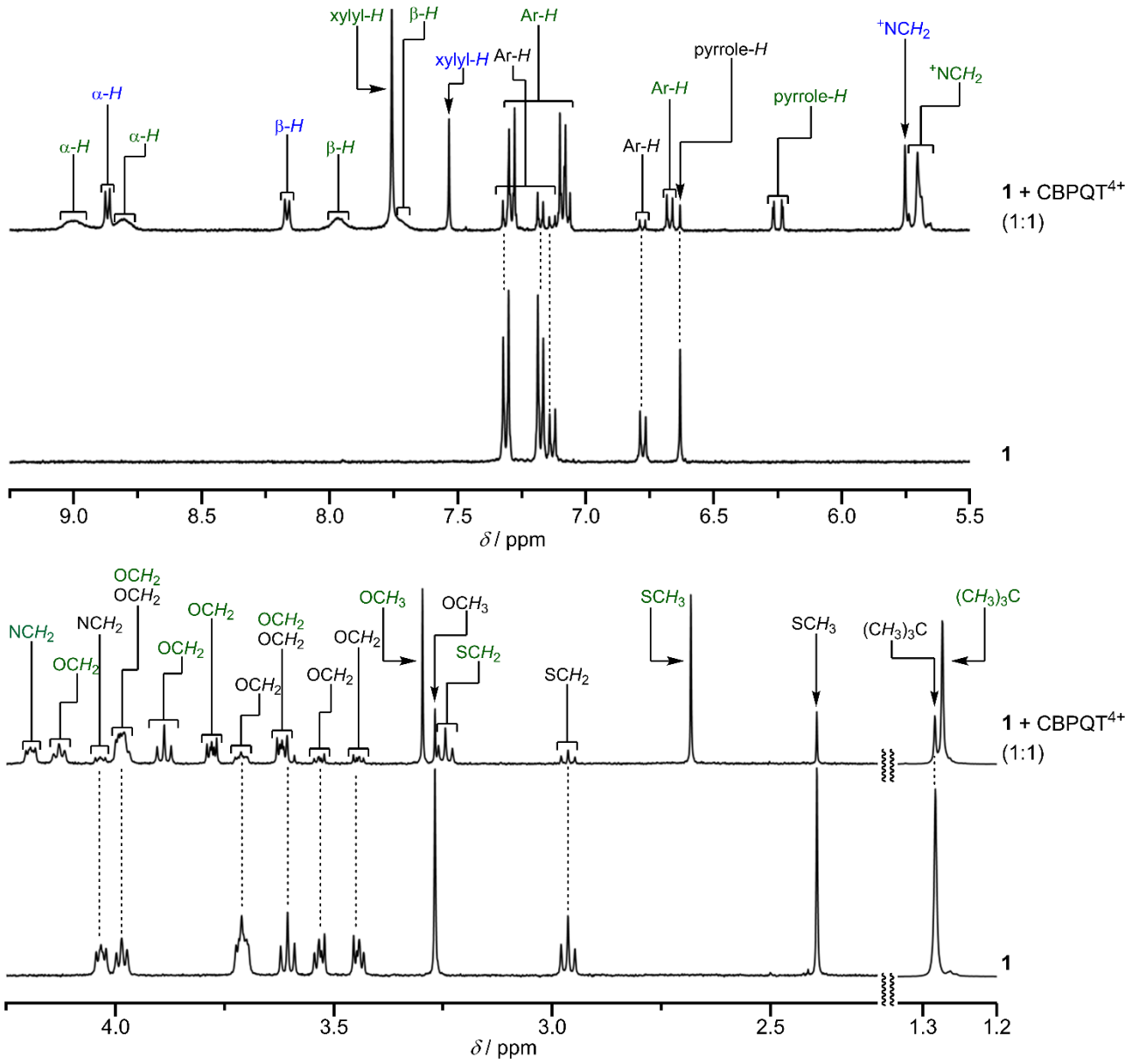

Fig. 4 Partial ^{1}H NMR spectra (400 MHz, 298 K, CD_3CN, 2 mM) of the semidumbbell **1** and an equilibrated 1:1 mixture of **1** and CBPQT^{4+}, where the assignments in black are blue are associated with the uncomplexed semidumbbell **1** and CBPQT^{4+}, respectively, while the assignments in green are associated with the [2]pseudorotaxane **1**⊂CBPQT^{4+}. The region from 1.20 to 1.32 ppm is scaled down to clarify the separation and height of the two $(CH_3)_3C$ signals.

Taken all together, these findings clearly indicate that the [2]rotaxane **2**$^{4+}$ almost exclusively exists as the translational isomer **2**•MPTTF^{4+} in which CBPQT^{4+} resides around the MPTTF station in CD_3CN at 298 K.

Further support for the formation of the [2]pseudorotaxane **1**⊂CBPQT^{4+} came from a comparison (Fig. 4) of the ^{1}H NMR spectra (400 MHz, 298 K) of the semidumbbell **1** and a 1:1 mixture of **1** and CBPQT^{4+} recorded in CD_3CN at 298 K.

The ^{1}H NMR spectrum (400 MHz) of an equilibrated 1:1 mixture of the semidumbbell **1** and CBPQT^{4+} recorded in CD_3CN at 298 K revealed three sets of signals, because of slow exchange between the complexed (*i.e.* **1**⊂CBPQT^{4+}) and uncomplexed species (*i.e.* **1** and CBPQT^{4+}) on the ^{1}H NMR time scale. The uncomplexed semidumbbell **1** (Fig. 4, black assignments) and CBPQT^{4+} (Fig. 4, blue assignments) are easily identified in the ^{1}H NMR spectrum, as all the protons in these two compounds were found to resonate at their original positions. The third set of signals observed in the ^{1}H NMR spectrum (Fig. 4, green assignments) recorded of the equilibrated 1:1 mixture of the semidumbbell **1** and CBPQT^{4+} are all shifted relative to the signals for the uncomplexed **1** and CBPQT^{4+} and can be associated with the [2]pseudorotaxane **1**⊂CBPQT^{4+}. As for [2]rotaxane **2**$^{4+}$, exchange between the two [2]pseudorotaxanes **1**⊂CBPQT•MPTTF^{4+} and **1**⊂CBPQT•OP^{4+} take place rapidly on the ^{1}H NMR time scale (CD_3CN, 400 MHz) at 298 K. Using the

same analysis as carried out on the [2]rotaxane $\mathbf{2}^{4+}$, it can be concluded that the [2]pseudorotaxane $\mathbf{1}\subset CBPQT^{4+}$ almost exclusively exists as the translational isomer $\mathbf{1}\subset CBPQT\bullet MPTTF^{4+}$ in CD_3CN at 298 K. The most diagnostic evidence which indicates that $CBPQT^{4+}$ encircles the MPTTF station is the downfield shift of the resonance for the SMe protons. This signal is observed as a singlet at δ = 2.68 ppm in $\mathbf{1}\subset CBPQT^{4+}$, compared with a singlet resonating at δ = 2.39 ppm in the uncomplexed semidumbbell **1**. The pyrrole-*H* protons also show significant shift upon complexation with $CBPQT^{4+}$. In the semidumbbell **1**, the two pyrrole-*H* protons were found resonating as a singlet at δ = 6.63 ppm, whereas in $\mathbf{1}\subset CBPQT^{4+}$, they were observed resonating as an AB system (J_{AB} = 2.0 Hz) at δ = 6.23 and 6.27 ppm. This finding is in perfect agreement with the results obtained from the ^{1}H NMR spectroscopic investigations (*vide supra*) of the [2]rotaxane $\mathbf{2}^{4+}$, where the pyrrole-*H* protons were found as an AB system (J_{AB} = 2.0 Hz) resonating at δ = 6.22 and 6.25 ppm.

Binding studies

To estimate the distribution of translational isomers present in the [2]pseudorotaxane $\mathbf{1}\subset CBPQT^{4+}$ and the [2]rotaxane $\mathbf{2}\bullet MPTTF^{4+}$, binding affinities for the formation of $\mathbf{1}\subset CBPQT^{4+}$ and two model host-guest systems $\mathbf{9}\subset CBPQT^{4+}$ and $\mathbf{10}\subset CBPQT^{4+}$ (Fig. 3) were compared. The MPTTF model compound **9** was synthesised as outlined in Scheme S1†. Mixing **9** with equimolar amounts of $CBPQT^{4+}$ in MeCN at 298 K leads to the production (Scheme S2†) of the [2]pseudorotaxane $\mathbf{9}\subset CBPQT^{4+}$, as indicated by the immediate appearance of a green-coloured solution. The UV-Vis-NIR spectrum (Fig. S2†) recorded of this solution showed a broad absorption band at 815 nm as a result of the CT interactions that occur when the MPTTF unit is located inside $CBPQT^{4+}$. The UV-Vis-NIR dilution method[59] (see ESI) was used to determine (Table 1) the binding constants (K_a) and the Gibbs free energies ($\Delta G°$) for the formation of the 1:1 complexes $\mathbf{1}\subset CBPQT^{4+}$ and $\mathbf{9}\subset CBPQT^{4+}$, respectively, in MeCN at 298 K, while the K_a and $\Delta G°$ values for the formation of $\mathbf{10}\subset CBPQT^{4+}$ were taken from the literature.[27]

A comparison of the thermodynamic data obtained for the complexation between $CBPQT^{4+}$ and the MPTTF derivative **9** and the OP derivative **10**, respectively, reveals that the binding affinity between $CBPQT^{4+}$ and the MPTTF station is four orders of magnitude higher relative to the binding affinity between $CBPQT^{4+}$ and the OP station in MeCN at 298 K. This observation clearly suggest that both the [2]pseudorotaxane $\mathbf{1}\subset CBPQT^{4+}$ and the [2]rotaxane $\mathbf{2}^{4+}$ almost exclusively (*vide supra*) will exist as the translational isomers $\mathbf{1}\subset CBPQT\bullet MPTTF^{4+}$ and $\mathbf{2}\bullet MPTTF^{4+}$, respectively, in which the MPTTF station is located inside the cavity of $CBPQT^{4+}$. Although the semidumbbell **1** contains two potential stations for $CBPQT^{4+}$ to reside around, it was found that the binding constant for the formation of $\mathbf{1}\subset CBPQT^{4+}$ was slightly lower as compared to the binding constant for the formation of $\mathbf{9}\subset CBPQT^{4+}$. This observation can most likely be accounted for by the fact that the large bulky stopper group present in **1** weakness the effect of stabilising [C–H···O] hydrogen bonding interactions between the α-*H* pyridinium protons of $CBPQT^{4+}$ and the oxygen atoms present in the diethyleneglycol chain connecting the MPPTF and the OP units.[§8]

Table 1 Binding constants (K_a) and derived free energies of complexation ($\Delta G°$) between $CBPQT^{4+}$ and the semidumbbell **1**, the two model compounds **9** and **10**[27] in MeCN at 298 K

Complex	λ_{max} [nm]	K_a [M^{-1}][a,c]	$\Delta G°$ [kcal mol^{-1}][c]
$\mathbf{1}\subset CBPQT^{4+}$ [b]	816	15000 ± 3000	–5.7 ± 0.1
$\mathbf{9}\subset CBPQT^{4+}$ [b]	815	26000 ± 7000	–6.0 ± 0.2
$\mathbf{10}\subset CBPQT^{4+}$ [d]	—	16 [e]	–1.7 [e]

[a] The K_a values reported are for the tetrakis(hexafluorophosphate) ($4PF_6^-$) salt of $CBPQT^{4+}$. [b] The K_a values for **1** and **9** were determined (see ESI) by the UV-Vis-NIR dilution method using the MPTTF/$CBPQT^{4+}$ CT band at λ_{max} as probes.[59] [c] The errors on the K_a and $\Delta G°$ values were obtained using the methods described by Nygaard *et al.*[59] with ΔT = 1 K, Δc = 3% and ΔA = 0.5%. [d] The K_a value for **10** was obtained using NMR spectroscopy in CD_3CN at 298 K and is taken from the literature.[27] [e] No errors were reported.

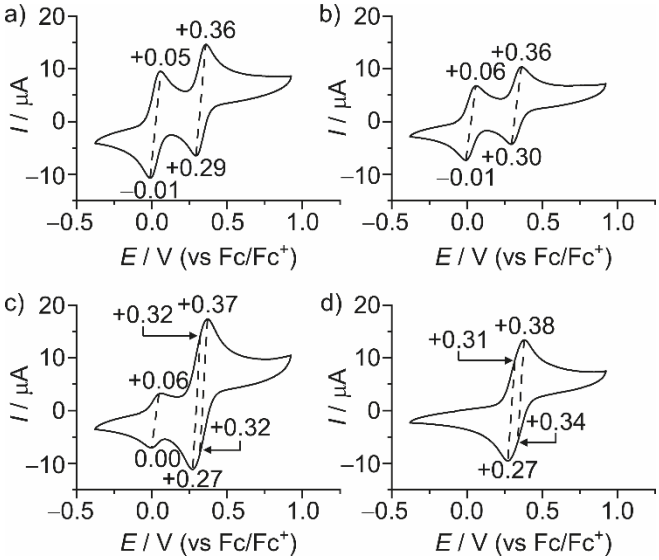

Fig. 5 Cyclic voltammograms of a) semidumbbell **1**, b) dumbbell **6**, c) a 1:2 mixture of **1** and $CBPQT^{4+}$ and d) [2]rotaxane $\mathbf{2}^{4+}$. The measurements were carried out at 298 K in nitrogen-purged solutions, 0.5 mM in MeCN with n-$Bu_4N\bullet PF_6$ as the electrolyte (0.1 M), a glassy carbon electrode as the working electrode and at a scan rate of 0.1 V s^{-1}.

Electrochemical investigations

The electrochemical properties of the semidumbbell **1**, the dumbbell **6**, a 1:2 mixture of **1** and $CBPQT^{4+}$ and the [2]rotaxane $\mathbf{2}^{4+}$ were investigated using cyclic voltammetry (CV). The cyclic voltammograms (CVs) were all recorded (Fig. 5) in nitrogen-purged MeCN at 298 K, and the obtained half-wave potentials ($E_{1/2}$) are summarised in Table 2, together with the corresponding anodic and cathodic peak potentials, *i.e.* E_{ox} and E_{red}, respectively. The CVs of the semidumbbell **1** (Fig. 5a) and the dumbbell **6** (Fig. 5b) shows both two mono-electronic reversible redox-waves associated with the two oxidation processes of the MPTTF unit (*i.e.* MPTTF → $MPTTF^{+\bullet}$ and $MPTTF^{+\bullet}$ → $MPTTF^{2+}$). A comparison of the results (Table 2) reveals that both the first and second redox-wave in the semidumbbell **1** and the dumbbell **6** take place at identical potentials when errors are taken into account. These observations indicate that the exchange of

Table 2 Electrochemical data for the semidumbbell **1**, the dumbbell **6**, a 1:2 mixture of **1** and CBPQT^{4+} and the [2]rotaxane **2**$^{4+}$ obtained by cyclic voltammetry[a] (CV) at 298 K in MeCN (*vs.* Fc/Fc^{+})

Compound	E_{ox}^1 [V][b]	E_{red}^1 [V][c]	$E_{1/2}^1$ [V][d]	E_{ox}^2 [V][b]	E_{red}^2 [V][c]	$E_{1/2}^2$ [V][d]	E_{ox}^3 [V][b]	E_{red}^3 [V][c]	$E_{1/2}^3$ [V][d]
1	+0.05	–0.01	+0.02	+0.36	+0.29	+0.33	–	–	–
6	+0.06	–0.01	+0.03	+0.36	+0.30	+0.33	–	–	–
1 + CBPQT^{4+}	+0.06	+0.00	+0.03	+0.32	+0.27	+0.30	+0.37	+0.32	+0.35
2^{4+}	+0.31	+0.27	+0.29	+0.38	+0.34	+0.36	–	–	–

[a] CV measurements of **1**, **6**, a mixture of **1** and CBPQT•4PF$_6$ (1:2) and **2**•4PF$_6$ in nitrogen-purged solutions (0.5 mM in MeCN) were conducted with 0.1 M *n*-Bu$_4$NPF$_6$ as the electrolyte, a glassy carbon electrode as the working electrode, a Pt counter electrode and with a scan rate of 0.1 V s^{-1}; E_{ox}, E_{red} and $E_{1/2}$ values *vs.* Fc/Fc^{+} and the estimated errors on the *E* values are ± 0.01 V. [b] Anodic oxidation peak. [c] Cathodic reduction peak. [d] Half-wave potential, $E_{1/2} = (E_{ox} + E_{red})/2$.

an SMe with an SEt group does not affect the redox properties of the MPTTF unit.

While the two mono-electronic redox-waves in the dumbbell **6** are well separated, they occur (Fig. 5d and Table 2) at two very close potentials (+0.29 and +0.36 V *vs.* Fc/Fc^{+}) in the [2]rotaxane **2**$^{4+}$. The shift of +0.26 V toward a more positive potential for the first redox-wave ($E_{1/2}^1$) in the [2]rotaxane **2**$^{4+}$ relative to the dumbbell **6**, clearly indicate that the MPTTF unit is encircled by CBPQT^{4+}.§9 The rather large anodically shift in the first redox-wave can be explained based on electrostatic repulsion and the strong CT interaction taking place between the MPTTF unit and the two electron-accepting bipyridinium moieties in CBPQT^{4+}.

A comparison between the second redox-wave ($E_{1/2}^2$) of the dumbbell **6** and the [2]rotaxane **2**$^{4+}$, reveals that the second oxidation process of the MPTTF unit in the [2]rotaxane **2**$^{4+}$ take place at a potential that is only slightly more positive ($\Delta E_{1/2}^2$ = +0.03 V) than the same process in the dumbbell **6**. This indicates that upon oxidation of the MPTTF unit to MPTTF$^{+\bullet}$, the CBPQT^{4+} ring will leave the mono-oxidised MPTTF unit producing **2**•OP^{5+}/$^{1\bullet}$ in which CBPQT^{4+} encircles the OP station (Scheme S4†), whereafter the non-encircled MPTTF$^{+\bullet}$ unit in **2**•OP^{5+}/$^{1\bullet}$ is oxidised to MPTTF^{2+} to give **2**•OP^{6+} at nearly the same potential as observed in the dumbbell **6**.

A more complex situation arises in the case of the [2]pseudorotaxane **1**⊂CBPQT^{4+} (Fig. 5c) since it is in equilibrium with its free components (*i.e.* **1** and CBPQT^{4+}). Therefore, the electrochemical characterisation of **1**⊂CBPQT^{4+} was carried out in a solution containing the semidumbbell **1** (0.5 mM) and two equiv. of CBPQT^{4+}. Under these conditions, it can be calculated§10 that the fraction (89%) of the [2]pseudorotaxane **1**⊂CBPQT^{4+} is very large compared to the small amount (11%) of uncomplexed semidumbbell **1**.

Although **1**⊂CBPQT^{4+} is in large excess, the presence of the uncomplexed semidumbbell **1** is still evident in the CV recorded (Fig. 5c) of the 1:2 mixture of **1** and CBPQT^{4+}, since the CV shows three redox-waves. The first redox-wave at $E_{1/2}$ = +0.06 V *(vs.* Fc/Fc^{+}) appears at the same potential as the first redox-wave (+0.05 V *vs.* Fc/Fc^{+}) for the semidumbbell **1** when errors are taken into account. Consequently, this process can be associated with the first oxidation of the MPTTF unit in the uncomplexed semidumbbell **1** present in the 1:2 mixture of **1** and CBPQT^{4+}. The second redox-wave observed at $E_{1/2}$ = +0.30 V can be assigned to the coincidence of the second oxidation of the MPTTF unit in the uncomplexed semidumbbell **1** and the first oxidation of the MPTTF unit in **1**⊂CBPQT^{4+}, while the third redox-wave observed at $E_{1/2}$ = +0.35 V can be assigned to the second oxidation of the MPTTF unit in **1**⊂CBPQT^{4+}. Since the two redox-waves at $E_{1/2}$ = +0.30 and +0.35 V assigned to the two oxidation processes of **1**⊂CBPQT^{4+} appear at the same potentials (Table 2) as those observed for the [2]rotaxane **2**$^{4+}$, it can be concluded that the CBPQT^{4+} ring also in the case of the [2]pseudorotaxane **1**⊂CBPQT^{4+} will leave the MPTTF unit after its first oxidation producing **1**⊂CBPQT•OP^{5+}/$^{1\bullet}$ in which CBPQT^{4+} encircles the OP station (Scheme S5†), followed by a second oxidation of **1**⊂CBPQT•OP^{5+}/$^{1\bullet}$ to give **1**⊂CBPQT•OP^{6+}.

The fact that the [2]pseudorotaxane **1**⊂CBPQT^{4+} shows electrochemical behaviour similar to that of the [2]rotaxane **2**$^{4+}$ clearly indicates that the CBPQT^{4+} ring remains around the semidumbbell on the ~10 s timescale of the CV experiment.

Kinetic investigations of 1⊂CBPQT^{4+}

As the complexation/decomplexation between the semidumbbell **1** and CBPQT^{4+} was found (*vide supra*) to be in slow exchange on the ^{1}H NMR time scale at 298 K, it is evident that the combination of the SMe group and the TDEG substituent constitute a steric/kinetic barrier for CBPQT^{4+}. This observation suggests that the [2]pseudorotaxane **1**⊂CBPQT•MPTTF^{4+} may be isolated as a "rotaxane-like" complex.[58] By employing flash column chromatography, it was possible to isolate **1**⊂CBPQT•MPTTF^{4+} as its PF_6^- salt, which immediately after its isolation was dissolved in MeCN and stored at 232 K.

The decomplexation of **1**⊂CBPQT•MPTTF^{4+}, where CBPQT^{4+} moves from the MPTTF unit over the SMe/TDEG barrier to form uncomplexed **1** and CBPQT^{4+}, is a unimolecular reaction and can accordingly be expected to follow first-order kinetics.

Initially, the isolated sample of **1**⊂CBPQT•MPTTF^{4+} in MeCN was heated§11 from 232 K to room temperature, whereafter the decomplexation process (Fig. 6a) was monitored at 298 K using the decrease (Fig. S4†) in the MPTTF/CBPQT^{4+} CT band (814 nm) as the probe. The data points were collected in the early stage of the experiment where the reverse process (*i.e.* complexation) is not yet occurring to any significant extent. After 100 s, a flattening of the curve was observed (Fig. 6b). Consequently, only the data from 0–100 s was used to determine the rate constant (k_d) for the decomplexation process. The selected experimental data were subjected to a first-order analysis, and the straight line obtained (Fig. 6b, red data) by plotting ln*A* against time (*t*) confirmed the first-order nature of the decomplexation process. The rate constant k_d and the corresponding free energy of activation§12 ($\Delta G^{\ddagger}_d$) were obtained directly from the slope of this straight line providing a k_d value of 1.485 ± 0.013 × 10^{-4} s^{-1} and a $\Delta G^{\ddagger}_d$ value of 22.70 ± 0.02 kcal mol^{-1} for the decomplexation process in MeCN at 298 K.§13,60

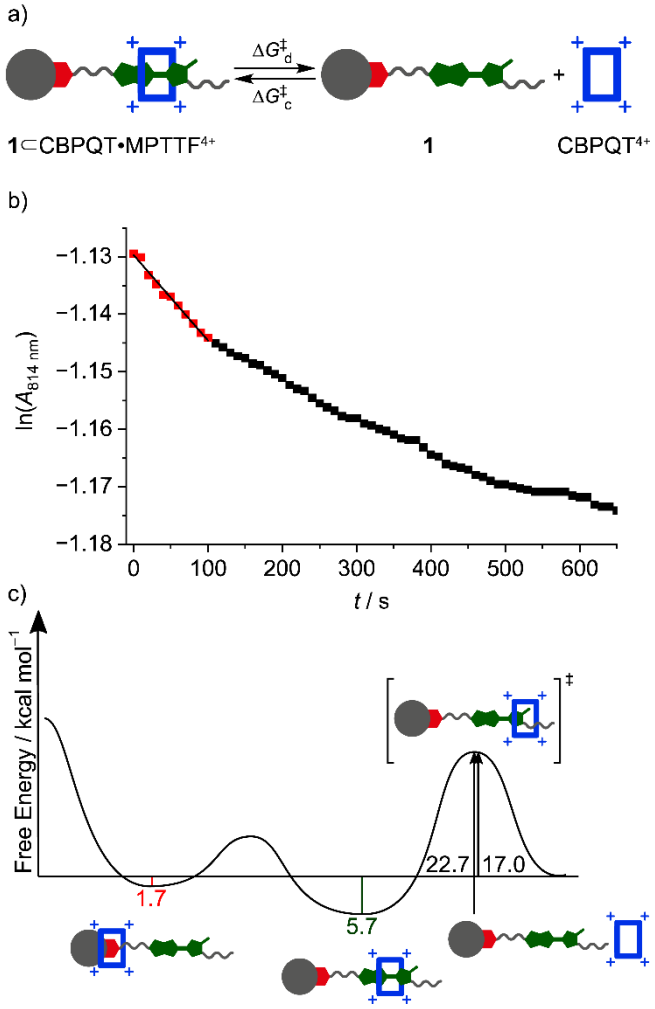

Fig. 6 a) A cartoon representation illustrating the decomplexation/complexation between the [2]pseudorotaxane **1**⊂CBPQT•MPTTF^{4+} and the uncomplexed species **1** and CBPQT^{4+}. b) Plot of ln*A* against *t* at 298 K for the decomplexation (d) of CBPQT^{4+} from **1**⊂CBPQT•MPTTF^{4+} by using the absorption (*A*) at 814 nm as the probe. The data points were collected in the early stage of the experiments where the complexation (c) process is not yet occurring to any significant extent and the red data points have been fitted by the best straight line, giving a correlation coefficient of 0.98, indicating that first order kinetic is in operation. The slope of the line gives the rate constant k_d, according to relationship $\ln A = -k_d t$. c) Energy diagram for the movement of CBPQT^{4+} away from the MPTTF unit in the [2]pseudorotaxane **1**⊂CBPQT•MPTTF^{4+} in MeCN at 298 K.

Since the free energy of complexation ($\Delta G°$) between the semidumbbell **1** and CBPQT^{4+} has been determined (Table 1), the corresponding free energy of activation for the complexation (*i.e.* $\Delta G^{‡}_c$) can be calculated by subtracting $-\Delta G°$ from $\Delta G^{‡}_d$ to give a $\Delta G^{‡}_c$ value of 17.0 kcal mol^{-1} ((22.7–5.7) kcal mol^{-1}) for the complexation between the semidumbbell **1** and CBPQT^{4+} in MeCN at 298 K (Fig. 6c). Consequently, it can be concluded that the energy of the transition state for the movement of CBPQT^{4+} over the SMe/TDEG barrier is 17.0 kcal mol^{-1} and it seems conceivable that the transition state structure (Fig. 6c) is a strained one in which the CBPQT^{4+} ring is forced up against the SMe and TDEG groups.[27]

Chemical oxidation of 2^{4+} and 1⊂CBPQT^{4+}

While the electrochemical investigations indicate that **2**•OP^{6+} and **1**⊂CBPQT•OP^{6+} are produced upon di-oxidation of **2**•MPTTF^{4+} and **1**⊂CBPQT•MPTTF^{4+}, respectively, ^{1}H NMR spectroscopy was used to confirm their formation.

Ten equiv. of the oxidising agent tris(*p*-bromophenyl)ammoniumyl hexachloroantimonate ($TBPASbCl_6$) were added to either a solution of the [2]rotaxane **2**•MPTTF^{4+} in CD_3CN at 298 K or the [2]pseudorotaxane **1**⊂CBPQT•MPTTF^{4+}, produced by allowing a 1:2 mixture of **1** and CBPQT^{4+} in CD_3CN to equilibrate for 10 h at 298 K,[§14] whereafter ^{1}H NMR spectra were recorded as fast as possible (*ca.* 10–15 min) after adding $TBPASbCl_6$.

Following oxidation, the observations of significant shifts to all the protons in the ^{1}H NMR spectra are consistent with the formation of the MPTTF^{2+} dication and the production of the translational isomers in which the CBPQT^{4+} ring encircles the OP station. In the ^{1}H NMR spectrum (Fig. 7, top) of the oxidised [2]rotaxane **2**$^{6+}$, the protons associated with the pyrrole-*H* protons are downfield shifted (δ = 8.21 ppm) relative to their position in which they are found resonating in the neutral [2]rotaxane **2**$^{4+}$ (δ = 6.22 and 6.25 ppm, Fig. 7, bottom). In the case of the oxidised [2]pseudorotaxane **1**⊂CBPQT^{6+}, the protons associated with the pyrrole-*H* protons are downfield shifted (δ = 8.21 ppm, Fig. S6†) compared to their position in which they are found resonating in the neutral [2]pseudorotaxane **1**⊂CBPQT^{4+} (δ = 6.23 and 6.27 ppm, Fig. S6†). Previous studies[25] have shown that such behaviour is fully consistent with the formation of the MPTTF^{2+} dication and, hence, the formation of the oxidised [2]rotaxane **2**$^{6+}$ and [2]pseudorotaxane **1**⊂CBPQT^{6+}, respectively, upon addition of $TBPASbCl_6$.

Evidence for the movement of the CBPQT^{4+} ring away from the oxidised MPTTF^{2+} unit is made obvious from the dramatic shifts in the resonances associated with the OP-H_b protons (Schemes 2 and 3) in the oxidised [2]rotaxane **2**$^{6+}$ and [2]pseudorotaxane **1**⊂CBPQT^{6+}, as compared to their positions in **2**•MPTTF^{4+} and **1**⊂CBPQT•MPTTF^{4+}, respectively.

In **2**•MPTTF^{4+} (Fig. 7, bottom) and **1**⊂CBPQT•MPTTF^{4+} (Fig. S6†), the OP-H_b protons appear as doublets (J = 8–9 Hz) resonating at δ = 6.68 and 6.67 ppm, respectively. Upon oxidation, the signals for the OP-H_b protons experience large upfield shifts to δ = 2.52 (**2**$^{6+}$) and 2.53 (**1**⊂CBPQT^{6+}) ppm, respectively, on account of the anisotropic shielding effect that occurs when the OP station is positioned inside the CBPQT^{4+} ring. Examination of the ^{1}H correlation spectroscopy (COSY) spectra for **1**⊂CBPQT^{6+} (Fig. S7†) and **2**$^{6+}$ (Fig. S8†) and recorded in CD_3CN at 298 K in both cases clearly displays through-bond scalar coupling between the shielded OP-H_b and OP-H_a protons. Consistently, the protons associated with the methylene group (*i.e.* –O–CH_2–) attached directly to the encircled OP station in **2**$^{6+}$ and **1**⊂CBPQT^{6+} are also significantly shielded (Fig. 7 and Fig. S6†) and appear both at δ = 1.52 ppm, and show through-bond scalar coupling to the neighbouring methylene group present in glycol chain.[§15] Overall, these observations unambiguously prove that **2**•OP^{6+} and **1**⊂CBPQT•OP^{6+} are produced upon di-oxidation of **2**•MPTTF^{4+} and **1**⊂CBPQT•MPTTF^{4+}, respectively.

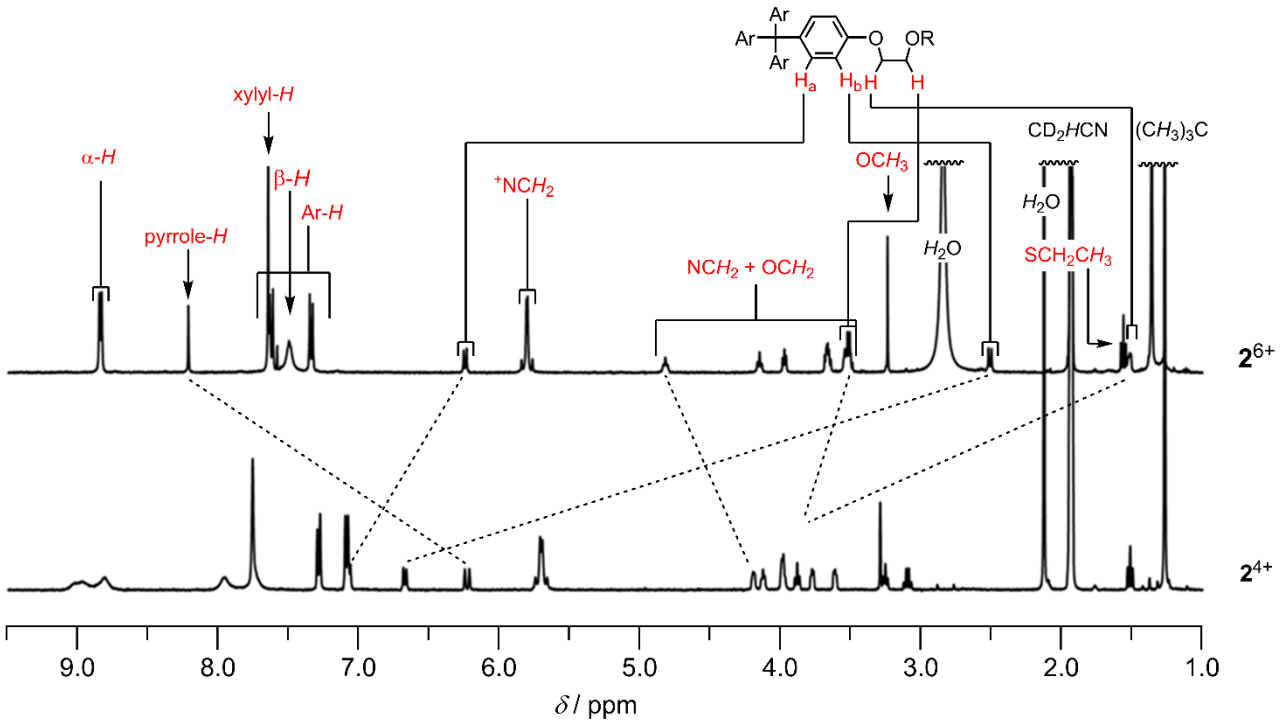

Fig. 7 Partial ^{1}H NMR spectra (400 MHz, 298 K, CD_3CN, 2 mM) recorded of the [2]rotaxane $\mathbf{2}^{4+}$ (bottom) and the oxidised [2]rotaxane $\mathbf{2}^{6+}$ (top). $\mathbf{2}^{6+}$ was generated by adding ten equiv. of $TBPASbCl_6$ to $\mathbf{2}^{4+}$. The $(CH_3)_3C$, CD_2HCN and H_2O signals are not shown in their full height.

After successful determination of the switching mechanism of **2**•MPTTF^{4+} and **1**⊂CBPQT•MPTTF^{4+}, the next step was to probe the stability of **2**•OP^{6+} and **1**⊂CBPQT•OP^{6+} on a longer timescale.

Initially, experiments were carried out on **2**•OP^{6+} in CD_3CN at 298 K. It was found that **2**•OP^{6+} over a period of 97 h decompose (Fig. S9†) without forming both **6**$^{2+}$ and CBPQT^{4+} when **2**•MPTTF^{4+} was oxidised with ten equiv. of $TBPASbCl_6$. To test whether it was the oxidised dumbbell **6**$^{2+}$ or CBPQT^{4+} that decomposed over time, a 1:1 mixture of the dumbbell **6** and CBPQT^{4+} was also oxidised (Fig. S9†) with ten equiv. of $TBPASbCl_6$. In this case, it was observed that the dumbbell **6**$^{2+}$ after 97 h was almost completely decomposed, while CBPQT^{4+} was unaffected by the oxidising environment.

In order to improve the stability of **2**•OP^{6+}, it was discovered that the addition of 100 equiv. of NH_4PF_6 increases the stability of the oxidised [2]rotaxane significantly. Therefore, ten equiv. of $TBPASbCl_6$ were added to a CD_3CN solution of **2**•MPTTF^{4+} at 298 K containing 100 equiv. of NH_4PF_6. The ^{1}H NMR spectra (Fig. S10†) recorded of this mixture after 1, 6, 23 and 48 h are almost identical, clearly indicating that the oxidised [2]rotaxane **2**$^{6+}$, is stable for more than 48 h under these conditions and that the CBPQT^{4+} ring is still located around the OP station.[§16] Consequently, it is evident that the CBPQT^{4+} ring does not possess enough thermal energy at 298 K to move across the combination of the MPTTF^{2+}/SEt/TDEG barrier, *i.e.* it is a stopper for CBPQT^{4+}.

Kinetic investigations of 1⊂CBPQT•OP^{6+}

Having found appropriate conditions to stabilise the oxidised [2]rotaxane **2**•OP^{6+} and dumbbell **6**$^{2+}$, the next step was to investigate the oxidised [2]pseudorotaxane **1**⊂CBPQT•OP^{6+} under the same conditions. While **2**•OP^{6+} was stable for more than 48 h and it was noticed that CBPQT^{4+} could not escape from the oxidised dumbbell component (Scheme S6†), the situation is different for **1**⊂CBPQT•OP^{6+}. In this case, it is evident that **1**⊂CBPQT•OP^{6+} is the kinetic product formed after oxidation of **1**⊂CBPQT•MPTTF^{4+} and that the CBPQT^{4+} ring subsequently deslips from the oxidised semidumbbell to produce the uncomplexed species **1**$^{2+}$ and CBPQT^{4+}, respectively (Fig. 8a).

The [2]pseudorotaxane **1**⊂CBPQT•MPTTF^{4+} was prepared by allowing a 1:2:100 mixture of the semidumbbell **1** (2 mM), CBPQT^{4+} (4 mM) and NH_4PF_6 (0.2 M) to equilibrate for 10 h in CD_3CN at 298 K before it was oxidised with ten equiv. of $TBPASbCl_6$. The ^{1}H NMR spectrum (400 MHz, 298 K) recorded of the oxidised solution reveals (Fig. S11†) that **1**⊂CBPQT•OP^{6+} is produced initially. When the oxidised solution is monitored over a longer time, it is clearly evident from the ^{1}H NMR spectra (Fig. S11†) that the signals arising from **1**⊂CBPQT•OP^{6+} (red assignments) decrease in intensity, while new signals corresponding to **1**$^{2+}$ (black assignments) and CBPQT^{4+} (blue assignments) simultaneously increases in intensity. For example, the signals associated with the OP-H_b and CBPQT^{4+} β-*H* protons in **1**⊂CBPQT•OP^{6+} resonating at δ = 2.58 and 7.46 ppm, respectively, decrease in intensity, while the same signals for the uncomplexed species **1**$^{2+}$ and CBPQT^{4+} that resonate at δ = 6.80 and 8.18 ppm, respectively, increase in intensity.

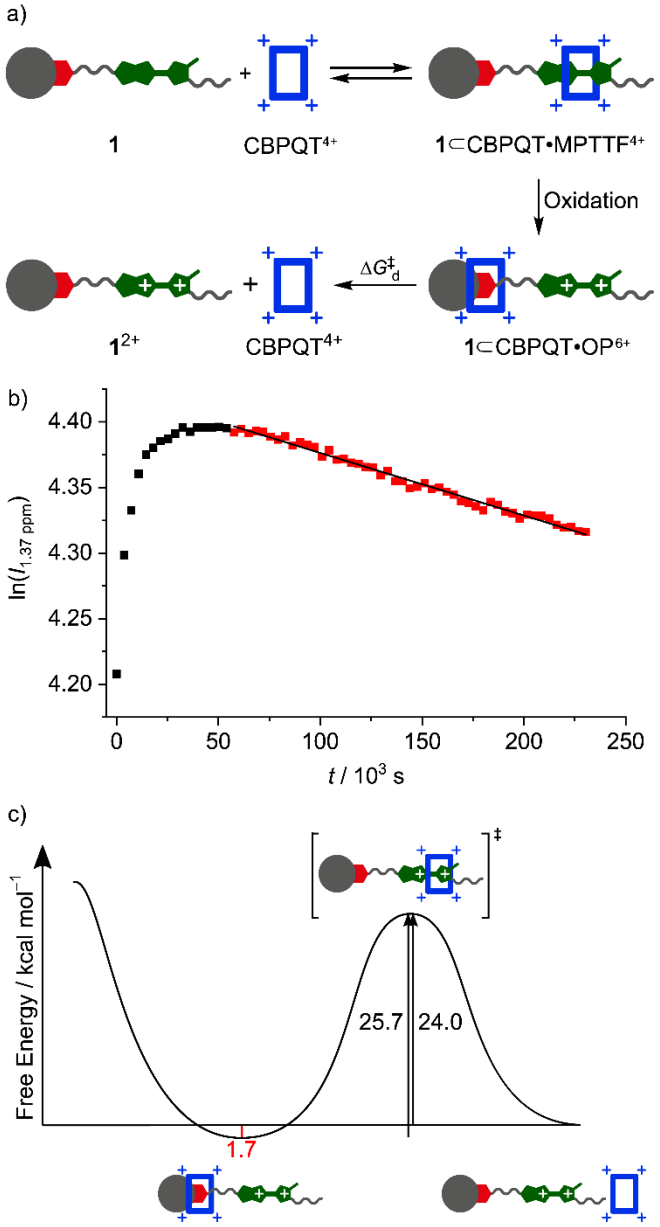

Fig. 8 A cartoon representation illustrating the oxidation process of **1**⊂CBPQT•MPTTF^{4+} leading initially to the formation of **1**⊂CBPQT•OP^{6+} followed by the slow production of uncomplexed semidumbbell **1**$^{2+}$ and CBPQT^{4+}. b) Plot of ln *I* against *t* at 294 K for the deslipping of CBPQT^{4+} from **1**⊂CBPQT•OP^{6+} by using the integral (*I*) at 1.37 ppm as the probe. The red data points have been fitted by the best straight line, giving a correlation coefficient of 0.989, indicating that first order kinetic are in operation. The slope of the line gives the rate constant k_d, according to relationship ln *I* = $-k_d t$. c) Energy diagram for the deslipping of CBPQT^{4+} from the OP moiety across the MPTTF^{2+} unit in the [2]pseudorotaxane **1**⊂CBPQT•OP^{6+} in CD_3CN at 298 K.

To quantify the size of the electrostatic barrier when CBPQT^{4+} moves from the OP station across the combined MPTTF^{2+}/SMe/TDEG barrier, ^{1}H NMR spectra (500 MHz) were recorded every hour for three days. An equilibrated mixture of **1**⊂CBPQT•MPTTF^{4+} and 100 equiv. of NH_4PF_6 were examined in CD_3CN at five different temperatures (294, 303, 308, 313 and 323 K) following oxidation with ten equiv. of $TBPASbCl_6$. First-order kinetic analysis was conducted using the signals for the C(CH_3)$_3$ and OCH_3 protons in both **1**⊂CBPQT•OP^{6+} and **1**$^{2+}$ as well as the xylyl-*H* protons in uncomplexed CBPQT^{4+} as probes[§17] with rate constants (k_d) obtained for the movement of CBPQT^{4+} over the MPTTF^{2+}/SMe/TDEG barrier in CD_3CN at 294, 303, 308, 313 and 323 K.[§18] A representative example at 294 K is shown in Fig. 8b, where the signal at δ = 1.37 ppm associated with the (CH_3)$_3$C protons in the oxidised [2]pseudorotaxane **1**⊂CBPQT•OP^{6+} is used as the probe. There is an initial lag period (black data points, Fig. 8b) before all **1**⊂CBPQT•MPTTF^{4+} is oxidised to **1**⊂CBPQT•OP^{6+} and the selected data points used to construct the linear plots (red data points, Fig. 8b and Fig. S12†) of ln *I* against time (*t*) were therefore the ones measured after the onset of a clear decrease in the intensity of the signals associated with **1**⊂CBPQT•OP^{6+}. Finally, the rate constant k_d and the corresponding energy of activation $\Delta G^{\ddagger}_d$ at each temperature were obtained as an average of the values obtained for each of the five different probes (Table S8†), which gave averaged $\Delta G^{\ddagger}_d$ values of 25.53 ± 0.02, 25.80 ± 0.02, 26.07 ± 0.02, 26.14 ± 0.02 and 26.37 ± 0.02 kcal mol^{-1} in CD_3CN at 294, 303, 308, 313 and 323 K, respectively. The enthalpic ($\Delta H^{\ddagger}_d$) and entropic ($\Delta S^{\ddagger}_d$) contributions (Table S9†) to the kinetic barrier were obtained by plotting (Fig. S13†) the barrier size ($\Delta G^{\ddagger}_d$) as a function of temperature (*T*). Interpolation of this plot gave a $\Delta G^{\ddagger}_d$ value of 25.7 ± 0.1 kcal mol^{-1} for the movement of CBPQT^{4+} from the OP station over the MPTTF^{2+}/SMe/TDEG barrier in CD_3CN at 298 K.

Providing that the binding affinity between the OP station and CBPQT^{4+} is not affected to any significant degree by oxidation of the MPTTF unit, an energy diagram for the deslipping of **1**⊂CBPQT•OP^{6+} can be constructed (Fig. 8c). Thus, based on a $\Delta G°$ value of –1.7 kcal mol^{-1} (Table 1) for the binding of CBPQT^{4+} to the OP station,[§19] it can be calculated that the energy of the transition state for the movement of CBPQT^{4+} over the MPTTF^{2+}/SMe/TDEG barrier is 24.0 kcal mol^{-1} ((25.7–1.7) kcal mol^{-1}) in CD_3CN at 298 K.

By comparing the energy of the transition state for the neutral [2]pseudorotaxane **1**⊂CBPQT^{4+} (Fig. 6) and the oxidised [2]pseudorotaxane **1**⊂CBPQT^{6+} (Fig. 8), it is evident that oxidation of the MPTTF unit to MPTTF^{2+} increases the energy barrier that the CBPQT^{4+} ring has to overcome in order for deslipping to occur with 7.0 kcal mol^{-1} ((24.0–17.0) kcal mol^{-1}). This increase in energy is most likely caused by the Coulombic repulsion that arises between the positive charged MPTTF^{2+} unit in **1**$^{2+}$ and the four positive charges present in the tetracationic CBPQT^{4+} ring. The magnitude of the electrostatic barrier (24.0 kcal mol^{-1}) for the movement of CBPQT^{4+} ring over the MPTTF^{2+} dication can be compared to the 2,6-dimethylpyridinium monocation (22.9 kcal mol^{-1}, CD_3CN, 298 K) determined in a CBPQT^{4+}-based [2]pseudorotaxane.[61]

Conclusions

We have reported the first measurement of the electrostatic barrier arising from the installation of two positive charges, by oxidation of the MPTTF station to MPTTF^{2+}, in a CBPQT^{4+}-based rotaxane. To make this measurement, we described the design and synthesis of a bistable [2]pseudorotaxane **1**⊂CBPQT•4PF_6

and a bistable [2]rotaxane **2**•4PF_6 both with monopyrrolotetrathiafulvalene (MPTTF) and oxyphenylene (OP) as stations and cyclobis(paraquat-*p*-phenylene) ($CBPQT^{4+}$) as the ring component. Our photophysical, electrochemically, and ^{1}H NMR spectroscopic studies reveal that the ground states of both exclusively exist as the translational isomers **1**⊂$CBPQT^{4+}$•$MPTTF^{4+}$ and **2**•$MPTTF^{4+}$, respectively, with $CBPQT^{4+}$ around the MPTTF station. Upon oxidation of the MPTTF station, **1**⊂$CBPQT^{4+}$•$MPTTF^{4+}$ and **2**•$MPTTF^{4+}$ can be switched to their corresponding translational isomers in which the OP station is located inside the $CBPQT^{4+}$ ring to produce **1**⊂$CBPQT^{4+}$•OP^{6+} and **2**•OP^{6+}, respectively. Our ^{1}H NMR spectroscopic studies revealed that in the case of the [2]rotaxane **2**•$MPTTF^{4+}$, the switching process was confined and that the switched [2]rotaxane **2**•OP^{6+} was stable for more than 48 h in CD_3CN at 298 K if 100 equiv. of NH_4PF_6 was added. However, in the case of the oxidised [2]pseudorotaxane **1**⊂$CBPQT^{4+}$•OP^{6+}, the $CBPQT^{4+}$ ring possesses enough thermal energy at 298 K to escape from the oxidised semidumbbell producing the uncomplexed species $\mathbf{1}^{2+}$ and $CBPQT^{4+}$, respectively. From our kinetic studies, we were able to determine the free energy of the transition state when $CBPQT^{4+}$ moves across either a neutral MPTTF unit (17.0 kcal mol^{-1}) or a di-oxidised $MPTTF^{2+}$ unit (24.0 kcal mol^{-1}) when they are substituted with a thiomethyl (SMe) and a thiodiethyleneglycol (TDEG) group. Consequently, it can be concluded that oxidation of the MPTTF unit to $MPTTF^{2+}$ increases the energy barrier that the $CBPQT^{4+}$ ring must overcome for deslipping to occur with 7.0 kcal mol^{-1}. This knowledge is believed to be important in the design of future systems, in which the movement of $CBPQT^{4+}$ needs to be controlled by electrochemical stimuli.

Experimental section

General

All chemicals are commercially available and were used as received unless otherwise stated. 2-(2-(4-[Tris(4-*tert*-butylphenyl)-methyl]phenoxy)ethoxy)ethyliodide (**3**),[33] 2-[4-(methylthio)-5-(2-(2-methoxyethoxy)ethylthio)-1,3-dithiol-2-ylidene]-5*H*-[1,3]dithiolo[4,5-*c*]pyrrole (**4**),[53] 2-[4-(ethylthio)-5-(2-(2-methoxyethoxy)ethylthio)-1,3-dithiol-2-ylidene]-5*H*-[1,3]dithiolo[4,5-*c*]pyrrole (**5**),[40] 1′′-[1,4-phenylene-bis(methylene)]bis(4,4′-bipyridinium) bis(hexafluorophosphate) (**7**•2PF_6),[54,62] cyclobis(paraquat-*p*-phenylene) tetrakis(hexafluorophosphate) ($CBPQT^{4+}$•4PF_6)[54,62] and 1-iodo-2-(2-methoxyethoxy)ethane (**11**)[63] were all prepared according to literature procedures. All reactions were carried out under an anhydrous nitrogen atmosphere. CH_2Cl_2 was distilled prior to use. DMF was dried over molecular sieves (4 Å) for at least 3 d prior to use. High pressure reactions were performed in a custom made teflon-tube, using a psika high pressure apparatus. Thin-layer chromatography (TLC) was carried out using aluminium sheets precoated with SiO_2 (Merck 60 F254) and visualised with UV light (254 nm) or I_2 vapor. Column chromatography was carried out using SiO_2 (Merck 60 F 0.040–0.063 mm). ^{1}H NMR and ^{13}C NMR spectra were recorded at 298 K (unless otherwise stated) at 400/500 MHz and 100 MHz, respectively, on a 400 MHz Bruker ADVANCED III spectrometer or on a 500 MHz Varian INOVA spectrometer using residual non-deuterated solvent as the internal standard. The solvent signals were assigned using Gottlieb *et al.*[64] All chemical shifts are quoted on a δ scale. The following abbreviations are used in listing the NMR spectra: s = singlet, bs = broad singlet, d = doublet, t = triplet, q = quartet, and m = multiplet. Melting points (Mp) were determined on a Büchi 353 melting point apparatus and are uncorrected. Electrospray ionisation mass spectrometry (ESI-MS) was performed on a Thermo Finnigan MAT SSQ710 single stage quadrupole mass spectrometer or a Bruker Avance III Daltonics MicrOTO-Q II ESI-Qq-TOF mass spectrometer. UV-Vis-NIR spectroscopic data were recorded on a Shimadzu UV-1601PC spectrophotometer or an Agilent Cary 5000 spectrophotometer. Cyclic voltammetry (CV) was carried out on an Autolab PGSTAT30 potentiostat. The CV cell consisted of a glassy carbon working electrode (WE), a Pt wire counter electrode (CE), and an $Ag/AgNO_3$ reference electrode (RE). The measurements were carried out in MeCN with *n*-Bu_4N•PF_6 (0.1 M) as the electrolyte and with a scan rate of 100 mV s^{-1} at 298 K. The WE was polished with an Al_2O_3 slurry prior to use and all solutions were degassed (N_2) prior to use. All redox potentials were measured against Ag/Ag^+ and converted into *vs.* ferrocene/ferrocenium (Fc/Fc^+). Elemental analyses were performed by Atlantic Microlabs, Inc., Norcross, GA, USA.

Semidumbbell 1. The MPTTF compound **4** (40.9 mg, 0.097 mmol) was dissolved in anhydrous DMF (10 mL) and degassed (N_2, 20 min) before NaH (60% w/w dispersion in mineral oil, 31.6 mg, 0.792 mmol) was added in one portion. The resulting red reaction mixture was stirred at room temperature for 10 min before 2-(2-(4-[tris(4-*tert*butylphenyl)methyl]phenoxy)ethoxy)ethyliodide (**3**), (67.7 mg, 0.096 mmol) was added in one portion, whereafter it was stirred at room temperature for 3 h. The reaction mixture was concentrated *in vacuo* and the resulting residue was re-dissolved in CH_2Cl_2 (50 mL) and washed with H_2O (3 × 25 mL). The combined aqueous phases were subsequently extracted with CH_2Cl_2 (25 mL) before the combined organic phases were dried ($MgSO_4$). Removal of the solvent gave a brown residue which was purified by column chromatography (60 mL SiO_2, 3 cm Ø, eluent: CH_2Cl_2:EtOAc, 9:1). The yellow band (R_f = 0.6 in CH_2Cl_2:EtOAc, 9:1) was collected and the solvent was evaporated affording **1** as a yellow solid. (69.0 mg, 72%). Mp 151–152.5 °C. ^{1}H NMR (400 MHz, CD_3CN, 298 K): δ 1.28 (s, 27H), 2.39 (s, 3H), 2.96 (t, J = 6.3 Hz, 2H), 3.27 (s, 3H), 3.43–3.45 (m, 2H), 3.52–3.54 (m, 2H), 3.60 (t, J = 6.3 Hz, 2H), 3.70–3.72 (m, 4H), 3.99 (t, J = 4.9 Hz, 2H), 4.02–4.04 (m, 2H), 6.63 (s, 2H), 6.78 (d, J = 8.9 Hz, 2H), 7.13 (d, J = 8.9 Hz, 2H), 7.18 (d, J = 8.6 Hz, 6H), 7.31 ppm (d, J = 8.6 Hz, 6H). MS (ESI): m/z 997 $[M]^+$. ^{13}C NMR (100 MHz, $CDCl_3$, 298 K): δ 19.2, 31.5, 34.5, 35.5, 50.9, 59.2, 63.3, 67.4, 70.1, 70.3, 70.6, 72.0, 77.4, 113.3, 119.1, 119.2, 124.2, 130.6, 130.9, 132.5, 140.2, 144.3, 148.5, 156.6 ppm.[§20] MS (HiRes-FT ESI): calcd for $C_{55}H_{67}NO_4S_6^+$: 997.3389; found: 997.3350. Anal. calcd for $C_{55}H_{67}NO_4S_6$: C, 66.16; H, 6.76; N, 1.40; S, 19.27; found: C, 66.04; H, 6.79; N, 1.37; S, 19.00.

[2]Pseudorotaxane 1⊂CBPQT•4PF$_6$. The yellow semidumbbell **1** (10 mg, 0.010 mmol) was dissolved in a minimum of CH_2Cl_2 (0.15 mL) and the colourless macrocycle CBPQT•4PF$_6$ (11 mg, 0.010 mmol) was dissolved in a minimum of Me_2CO (HPLC grade, 3.0 mL). Mixing the two solutions produced initially a yellow-coloured solution. Leaving the yellow solution to stand for 16 h at room temperature gave a green solution. The green solution was subjected to fast (< 5 min) flash column chromatography (25 mL SiO_2, 1.5 cm Ø) and the first yellow band containing the semidumbbell compound **1** was eluted with Me_2CO, whereupon the eluent was changed to Me_2CO (HPLC grade)/NH_4PF_6 (100:1 v/w). The green band was collected in a cold flask (cooled below 273 K) and the solvent was removed *in vacuo* (T < 273 K). The resulting green residue was dissolved immediately thereafter in an appropriate amount of MeCN/CD_3CN. Fast centrifuging (<30 s) followed by decantation of the solution was carried out to get rid of most NH_4PF_6. The resulting green solution was stored at 232 K until use (the following day). ^{1}H NMR (400 MHz, CD_3CN, 298 K): δ 1.27 (s, 27H), 2.68 (s, 3H), 3.25 (t, J = 6.4 Hz, 2H), 3.30 (s, 3H), 3.61–3.63 (m, 2H), 3.77–3.79 (m, 2H), 3.89 (t, J = 6.4 Hz, 2H), 3.97–4.00 (m, 4H), 4.12–4.14 (m, 2H), 4.19–4.21 (m, 2H), 5.66 and 5.73 (AB, J_{AB} = 13.6 Hz, 8H), 6.23 and 6.27 (AB, J_{AB} = 2 Hz, 2H), 6.68 (d, J = 8.2 Hz, 2H), 7.07 (d, J = 8.2 Hz, 2H), 7.09 (d, J = 8.8 Hz, 6H), 7.29 (d, J = 8.8 Hz, 6H), 7.74 (bs, 4H), 7.76 (s, 8H), 7.97 (bs, 4H), 8.81 (bs, 4H), 9.00 ppm (bs, 4H).

[2]Pseudorotaxane 1⊂CBPQT•OP^{6+}. Tris(*p*-bromophenyl)ammoniumyl hexachloroantimonate ($TBPASbCl_6$) (12.8 mg, 15.7 µmol) was added to a solution of the [2]pseudorotaxane **1**⊂CBPQT•4PF$_6$, produced by allowing a 1:2 mixture of **1** (1.42 mg, 1.42 µmol) and CBPQT^{4+} (3.12 mg, 2.83 µmol) in 0.2 M NH_4PF_6 solution in CD_3CN (0.73 mL) to equilibrate for 10 h at 298 K, whereafter a ^{1}H NMR spectrum of the formed **1**⊂CBPQT•OP^{6+} was recorded as fast as possible (*ca.* 4–5 min). ^{1}H NMR (400 MHz, CD_3CN, 298 K): δ 1.37 (s, 27H), 1.50–1.55 (m, 2H), 2.53 (d, J = 8.7 Hz, 2H), 3.07 (s, 3H), 3.24 (s, 3H), 3.50–3.56 (m, 4H), 3.63−3.70 (m, 4H), 3.92−3.99 (m, 2H), 4.16 (t, J = 6.3 Hz, 2H), 4.82 (t, J = 6.3 Hz, 2H), 5.79 and 5.82 (AB, J_{AB} (H,H) = 13.6 Hz, 8H), 6.25 (d, J = 8.7 Hz, 2H), 7.34 (d, J = 8.5 Hz, 6H), 7.50 (bs, 8H), 7.62 (d, J = 8.5 Hz, 6H), 7.65 (s, 8H), 8.21 (s, 2H), 8.84 ppm (d, J = 6.6 Hz, 8H).

Dumbbell 6. The MPTTF compound **5** (79.9 mg, 0.183 mmol) was dissolved in anhydrous DMF (12 mL) and degassed (N_2, 15 min) before NaH (60% w/w dispersion in mineral oil, 57.5 mg, 1.44 mmol) was added in one portion. The resulting red reaction mixture was stirred at room temperature for 10 min before 2-(2-(4-[tris(4-*tert*butylphenyl)methyl]phenoxy)ethoxy)ethyliodide (**3**) (132 mg, 0.188 mmol) was added in one portion, whereafter it was stirred at room temperature for 2.25 h. The reaction mixture was concentrated *in vacuo* before it was re-dissolved in CH_2Cl_2 (100 mL), washed with H_2O (3 × 50 mL) and dried ($MgSO_4$). Removal of the solvent gave a brown solid which was purified by column chromatography (60 mL SiO_2, 3 cm Ø, eluent: CH_2Cl_2). The yellow band (R_f = 0.4 in CH_2Cl_2) was collected, and the solvent evaporated affording **6** as a yellow/orange solid (144 mg, 78%). Mp 150–151 °C. ^{1}H NMR (400 MHz, CD_3CN, 298 K): δ 1.25 (t, J = 7.2 Hz, 3H), 1.28 (s, 27H), 2.84 (q, J = 7.2 Hz, 2H), 2.98 (t, J = 6.3 Hz, 2H), 3.27 (s, 3 H), 3.43–3.45 (m, 2H), 3.52–3.54 (m, 2H), 3.60 (t, J = 6.3 Hz, 2H), 3.70–3.72 (m, 4H), 3.97–3.99 (m, 2H), 4.02–4.04 (m, 2H), 6.63 (s, 2H), 6.77 (d, J = 8.2 Hz, 2H), 7.13 (d, J = 8.2 Hz, 2H), 7.17 (d, J = 8.2 Hz, 6H), 7.31 ppm (d, J = 8.2 Hz, 6H). ^{13}C NMR (100 MHz, $CDCl_3$, 298 K): δ 15.2, 30.6, 31.5, 34.5, 35.5, 50.8, 59.2, 63.2, 67.4, 70.1, 70.3, 70.6, 72.0, 77.4, 113.3, 119.1, 124.2, 126.6, 128.7, 130.9, 132.5, 140.2, 144.3, 148.5, 156.6 ppm.[§20] MS (ESI) m/z 1011 [M]$^+$, 413. MS (HiRes-FT ESI): calcd for $C_{56}H_{69}NO_4S_6^+$: 1011.3546; found: 1011.3520. Anal. calcd for $C_{56}H_{69}NO_4S_6$: C, 66.43; H, 6.87; N, 1.38; S, 19.00; found: C, 66.68; H, 6.79; N, 1.48; S, 18.79.

[2]Rotaxane 2•4PF$_6$. 1,1''-[1,4-Phenylene-bis(methylene)]bis(4,4'-bipyridinium)bis(hexafluorophosphate) (**7**•2PF$_6$) (936 mg, 1.32 mmol) and 1,4-bis(bromomethyl)benzene (**8**) (350 mg, 1.33 mmol) was added to a solution of the dumbbell **6** (331 mg, 0.327 mmol) in CH_2Cl_2 (0.5 mL), whereupon anhydrous DMF (5.5 mL) were added. The reaction mixture was transferred to a Teflon tube and subjected to 10 kbar pressure for 3 d at room temperature. The resulting dark green solution was directly subjected to column chromatography (200 mL SiO_2, 3 cm Ø) and unreacted dumbbell **6** was eluted with Me_2CO, whereupon the eluent was changed to Me_2CO/NH_4PF_6 (100:1 v/w) and the green band was collected. Most of the solvent was removed *in vacuo* (~ 10 mL) followed by addition of cold H_2O (0 °C, 30 mL). The suspension was cooled on an ice/water bath for 15 min, whereupon the resulting green precipitate was collected by filtration, washed with cold H_2O (0 °C, 3 × 3 mL) and Et_2O (3 × 3 mL) before being dried affording the [2]rotaxane **2**•4PF$_6$ as a green solid (125 mg, 18%). Mp > 235 °C. ^{1}H NMR (400 MHz, CD_3CN, 298 K): δ 1.27 (s, 27H), 1.52 (t, J = 7.4 Hz, 3H), 3.10 (q, J = 7.4 Hz, 2H), 3.26 (t, J = 6.5 Hz, 2H), 3.29 (s, 3H), 3.60–3.63 (m, 2H), 3.77–3.79 (m, 2H), 3.88 (t, J = 6.5 Hz, 2H), 3.97–4.00 (m, 4H), 4.11–4.14 (m, 2H), 4.18–4.20 (m, 2H), 5.69 and 5.72 (AB, J_{AB} = 13.4 Hz, 8H), 6.22 and 6.25 (AB, J_{AB} = 2 Hz, 2H), 6.67 (d, J = 8.8 Hz, 2H), 7.07 (d, J = 8.8 Hz, 2H), 7.09 (d, J = 8.4 Hz, 6H), 7.29 (d, J = 8.4 Hz, 6H), 7.75 (bs, 4H), 7.75 (s, 8H), 7.96 (bs, 4H), 8.80 (bs, 4H), 8.97 (bs, 2H), 9.05 ppm (bs, 2H). ^{13}C NMR (100 MHz, CD_3CN, 298 K): δ 15.8, 31.3, 31.6, 35.0, 36.4, 51.8, 58.9, 64.0, 65.7, 68.8, 70.9, 70.9, 71.1, 71.7, 72.6, 114.6, 114.9, 114.9, 117.0, 117.2, 125.5, 127.3, 131.2, 131.8, 132.9, 137.6, 141.2, 145.5, 147.4, 149.7, 157.4 ppm.[§20] MS (ESI): m/z 1011 [M – CBPQT•4PF$_6$]$^+$, 911 [M – 2PF$_6$]$^{2+}$, 559 [M – 3PF$_6$]$^{3+}$, 511 [M – 4PF$_6$]$^{3+}$. MS (HiRes-FT ESI): calcd for $C_{92}H_{101}F_{12}N_5O_4P_2S_6^+$: 910.7725; found: 910.7730. Anal. calcd for $C_{92}H_{101}F_{24}N_5O_4P_4S_6$: C, 52.29; H, 4.82; N, 3.31; S, 9.10; found: C, 52.05; H, 4.85; N, 3.50; S, 8.89.

[2]Rotaxane 2•OP^{6+}. Tris(*p*-bromophenyl)ammoniumyl hexachloroantimonate ($TBPASbCl_6$) (8.41 mg, 10.3 µmol) was added to a solution of the [2]rotaxane **2**•4PF$_6$ (2.73 mg, 1.29 µmol) in CD_3CN (650 µL), whereafter a ^{1}H NMR spectrum of the formed **2** •OP^{6+} was recorded. ^{1}H NMR (400 MHz, CD_3CN, 298 K): δ 1.37 (s, 27H), 1.51–1.54 (m, 2H), 1.57 (t, J = 7.3 Hz, 3H), 2.52 (d,

J = 8.0 Hz, 2H), 3.30 (s, 3H), 3.48–3.58 (m, 6H), 3.62–3.72 (m, 4H), 3.98 (t, *J* = 5.1 Hz, 2H), 4.15 (t, *J* = 6.2 Hz, 2H), 4.82 (t, *J* = 6.2 Hz, 2H), 5.79 and 5.82 (AB, J_{AB} = 13.5 Hz, 8H), 6.25 (d, *J* = 8.0 Hz, 2H), 7.34 (d, *J* = 8.5 Hz, 6H), 7.50 (bs, 8H), 7.62 (d, *J* = 8.5 Hz, 6H), 7.65 (s, 8H), 8.21 (s, 2H), 8.84 ppm (d, *J* = 6.7 Hz, 8H).

Model compound 9.§21 The MPTTF compound **4** (76.0 mg, 0.179 mmol) was dissolved in anhydrous DMF (10 mL) and degassed (N_2, 20 min) before NaH (60% w/w dispersion in mineral oil, 51.5 mg, 1.29 mmol) was added in one portion. The resulting red reaction mixture was stirred at room temperature for 10 min before 1-iodo-2-(2-methoxyethoxy)ethane (**11**) (38.5 mg, 0.167 mmol) dissolved in DMF (1 mL) was added in one portion, whereafter it was stirred at room temperature for 4.5 h. The reaction mixture was concentrated *in vacuo* and the resulting residue was re-dissolved in CH_2Cl_2 (100 mL), washed with H_2O (3 × 50 mL), dried ($MgSO_4$) and concentrated *in vacuo*. The resulting yellow residue was purified by multiple gradient column chromatography (60 mL SiO_2, 3 cm Ø, eluent: CH_2Cl_2:EtOAc, 9:1). The yellow band (R_f = 0.2 in CH_2Cl_2:EtOAc, 9:1) was collected and the solvent was evaporated affording **9** as an orange oil. (61.0 mg, 69%). ^{1}H NMR (400 MHz, CD_3CN, 298 K). δ = 2.43 (s, 3H), 2.99 (t, *J* = 6.3 Hz, 2H), 3.27 (s, 3H), 3.28 (s, 3H), 3.41–3.48 (m, 4H), 3.49–3.53 (m, 2H), 3.53–3.57 (m, 2H), 3.62 (t, *J* = 6.3 Hz, 2H), 3.65 (t, *J* = 5.2 Hz, 2H), 3.99 (t, *J* = 5.2 Hz, 2H), 6.65 ppm (s, 2H). ^{13}C NMR (100 MHz, CD_3CN, 298 K): δ 19.3, 36.4, 51.3, 59.0, 70.6, 71.0, 71.1, 71.6, 72.6, 72.6, 109.4, 114.7, 118.7, 118.7, 121.7, 125.2, 131.3 ppm.§20 MS (ESI): *m/z* 526 $[M+H]^+$. MS (HiRes-FT ESI): calcd for $C_{19}H_{28}NO_4S_6^+$: 526.0337; found: 526.0314. Anal calcd for $C_{19}H_{27}NO_4S_6$: C, 43.40; H, 5.18; N, 2.66; S, 36.59; found: C, 43.45; H, 5.04; N, 2.69; S, 36.44.

Kinetic experiments. The rate constant for the decomplexation of **1**⊂CBPQT•MPTTF^{4+} into **1** and CBPQT^{4+} were measured at 298 K using UV-Vis-NIR spectroscopy. Initially, the isolated [2]pseudorotaxane **1**⊂CBPQT•4PF_6 in a 232 K MeCN solution was transferred to a 3.0 mL cuvette (*l* = 1 cm) and quickly heated to room temperature, before being placed in the thermostated cell compartment of the UV-Vis-NIR spectrophotometer at 298 K. The movement was monitored by using the MPTTF/CBPQT^{4+} CT band (814 nm) as the probe. The data points collected in the early stage of the experiment (100 s) where the reverse process is not yet occurring in any significant extent were subjected to a first-order analysis by plotting ln*A* against *t* and fitted by the best straight line, giving a correlation coefficient of 0.98. The slope of the line gives the rate constant k_d, according to relationship $\ln A = -k_d t$.

The rate constants k_d for the decomplexation of **1**⊂CBPQT•OP^{6+} into **1**$^{2+}$ and CBPQT^{4+} were measured at different temperatures (294, 303, 308, 313 and 323 K) using ^{1}H NMR spectroscopy (500 MHz). The [2]pseudorotaxane **1**⊂CBPQT•MPTTF^{4+} was prepared by allowing a 1:2:100 mixture of the semidumbbell **1** (2 mM), CBPQT^{4+} (4 mM), and NH_4PF_6 (0.2 M) to equilibrate for 10 h in CD_3CN at 298 K before it was oxidised with ten equiv. of $TBPASbCl_6$ to give **1**⊂CBPQT•OP^{6+}. ^{1}H NMR spectra (500 MHz) were recorded every hour for 3 d. Initially, phase and baseline correction were performed on all spectra and each spectrum was normalised using the integral of TMS signal as internal standard. All signals that did not overlap with the H_2O/*H*DO signal or any other signals were integrated and used as probes. For each probe, a plot of ln*I* against *t*, where *I* is the integral of the signal in question and *t* is the time, was made, and a number of data points, *n*, after all **1**⊂CBPQT•MPTTF^{4+} was oxidised were fitted by the best straight line, giving correlation coefficients of 0.87–1.00. The slope of the line gives the rate constant k_d, according to relationship $\ln I = -k_d t$.

Conflicts of interest

There are no conflicts to declare.

Acknowledgements

This research was funded by The Danish Natural Science Research Council (FNU, project no. 11-106744 and 9040-00169B) and the Villum Foundation in Denmark and by the National Science Foundation (CHE-2105848) in the United States.

Notes and references

§1 A [2]catenane is a molecule composed of two interlocked macrocyclic components. The two macrocycles are not linked covalently to each other, rather, a mechanical bond holds them together and prevents their dissociation.[30]

§2 A [2]rotaxane is a molecule composed of a ring component and a dumbbell-shaped component. The ring component encircles the linear rodlike portion of the dumbbell-shaped component and is trapped mechanically around it by two bulky stoppers. Thus, the two components cannot dissociate from one another, although they are not linked covalently to each other.

§3 In the experiments conducted by Stoddart and coworkers, the bistable [2]rotaxane was immobilised on a silicon surface a pulling force of 145 pN was required to allow the CBPQT^{4+} ring to move across the TTF^{2+} unit. By combining spectroscopic and computational data, it was concluded that that the electrostatic barrier energy for the CBPQT^{4+} ring to cross the TTF^{2+} unit is 65 kcal mol^{-1}.[47]

§4 In a [2]pseudorotaxane[2] at least one of the stoppers on the dumbbell-shaped component is absent with the consequence that dissociation of the [2]pseudorotaxane into its two components can occur, and the equilibrium between the species is controlled by the free energy of complexation, *i.e.* a [2]pseudorotaxane is a 1:1 complex.

§5 The distinction between rotaxanes and pseudorotaxanes is far from being a straightforward one. When size-complementarity between the stoppers and the macrocyclic component is achieved, certain "rotaxanes" behave as pseudorotaxanes and can dissociate into their components under appropriate conditions. Thus, a specie which is a rotaxane at ambient temperature might well be a pseudorotaxane at elevated temperatures. Even a solvent change can turn a rotaxane into a pseudorotaxane at the same temperature.[46-49]

§6 In the literature, this stopper is usually called the tetraarylmethane stopper, however, it was found[27] that the oxyphenylene-part

of the stopper is also a recognition site for $CBPQT^{4+}$, hence we here denote the non-oxyphenylene part of the stopper as triarylmethyl.

§7 The K_{eq} value for the equilibrium between **2**•$MPTTF^{4+}$ and **2**•OP^{4+} was calculated using the relationship $K_{eq} = \exp[(-\Delta\Delta G°)/RT)]$ where $\Delta\Delta G° = \Delta G°$ (**10**⊂$CBPQT^{4+}$) − $\Delta G°$ (**9**⊂$CBPQT^{4+}$), R is the gas constant and T is the absolute temperature.

§8 It has previously been shown that attachment of glycol chains to the pyrrole moiety of the MPTTF unit stabilise the resulting [2]pseudorotaxanes with 0.3 kcal mol^{-1} as a result of [C–H···O] hydrogen bonding interactions taking place between the α-*H* pyridinium protons of $CBPQT^{4+}$ and the first and in particular the second oxygen atoms present in the glycol chains.[57]

§9 In a single station [2]rotaxane, containing only an MPTTF station in the dumbbell component and $CBPQT^{4+}$ as the ring component, the two monoelectronic redox-waves of the MPTTF unit was only separated by 0.04 V, and the first redox-wave in this single station [2]rotaxane was shifted 0.33 V toward more positive potential, compared to the same process in the corresponding dumbbell.[29]

§10 The calculation was carried out using a K_a value of 15000 M^{-1} for the complexation between **1** and $CBPQT^{4+}$ and intial concentrations of 0.5 mM and 1.0 mM for **1** and $CBPQT^{4+}$, respectively.

§11 For further details, see the Experimental section.

§12 The $\Delta G^{‡}$ value was calculated using the relationship $\Delta G^{‡} = RT\ln(kh/k_BT)$, where R is the gas constant, T is the absolute temperature, k is the rate constant, h is Planck's constant and k_B is the Boltzmann constant.

§13 The errors on the k and $\Delta G^{‡}$ values were calculated using the method described in Koumura *et al.*[58] with ΔT = 0.2 K, Δt = 0.1 s and ΔA = 0.05%.

§14 The [2]pseudorotaxane **1**⊂CBPQT•$MPTTF^{4+}$ was produce by mixing the semidumbbell **1** (2 mM) and $CBPQT^{4+}$ (4 mM) in CD_3CN at 298 K. The ^{1}H NMR spectrum (400 MHz, 298 K) recorded (Fig. S5†) of this solution revealed that the amount of the [2]pseudorotaxane **1**⊂CBPQT•$MPTTF^{4+}$ is 95%. By using a K_a value of 15000 M^{-1} for the complexation between **1** and $CBPQT^{4+}$, it can be calculated that the fraction of the [2]pseudorotaxane **1**⊂CBPQT•$MPTTF^{4+}$ under these conditions is 97%.

§15 In the ^{1}H NMR spectrum (Fig. S6†) of the oxidised [2]pseudorotaxane **1**⊂CBPQT•$MPTTF^{4+}$, small signals that can assigned to the oxidised semidumbbell $\mathbf{1}^{2+}$ is also observed. This observation can be accounted for by the fact that a minor amount of the semidumbbell **1** is not complexed to $CBPQT^{4+}$ before the 1:2 mixture of **1** and $CBPQT^{4+}$ is oxidised with $TBPASbCl_6$, see: note §14.

§16 The stability of **2**•OP^{6+} was established by comparing the integrals of the signals assigned to the OP-H_a and OP-H_b protons with the integrals for the tetramethylsilane (TMS) signal. Since no changes was observed, it can be concluded that the oxidised [2]rotaxane **2**•OP^{6+} is stable for more than 48 h in CD_3CN at 298 K in the presence of 100 equiv. of NH_4PF_6.

§17 These signals were found useful as probes since they do not overlap with other signals and because they originate from all three species (*i.e.* **1**⊂CBPQT•OP^{6+}, $\mathbf{1}^{2+}$ and $CBPQT^{4+}$) present during the experiments, for further information see ESI.

§18 At each temperature and for each probe first-order kinetics are observed to be obeyed (see Tables S3–S7†) when ln I is plotted against t, where I is the integral of the signal in question at time t. This outcome is a consequence of the fact that only deslipping can take place because of the very low affinity between the oxidised semidumbbell $\mathbf{1}^{2+}$ and $CBPQT^{4+}$.

§19 By using a K_a value of 16 M^{-1} (Table 1) for the complexation between the OP station and $CBPQT^{4+}$ and the initial concentrations for the semidumbbell **1** (2 mM) and $CBPQT^{4+}$ (4 mM), it can be calculated that the fraction of the oxidised [2]pseudorotaxane **1**⊂CBPQT•OP^{6+} is 6% at equilibrium under these conditions at 298 K.

§20 Signal(s) missing due to overlap or low intensity.

§21 See Scheme S1†.

1. E. Wasserman, *J. Am. Chem. Soc.*, 1960, **82**, 4433−4434.
2. G. Schill, *Catenanes, Rotaxanes, and Knots*, Academic Press, New York, 1971.
3. J.-M. Lehn, *Angew. Chem. Int. Ed. Engl.*, 1988, **27**, 89–112.
4. J.-M. Lehn, *Supramolecular Chemistry*, Wiley-VCH, Weinheim, Germany, 1 edn., 1995.
5. G. M. Whitesides and B. Grzybowski, *Science*, 2002, **295**, 2418–2421.
6. P. Thordarson, *Chem. Soc. Rev.*, 2011, **40**, 1305–1323.
7. E. J. Dale, N. A. Vermeulen, M. Juríček, J. C. Barnes, R. M. Young, M. R. Wasielewski and J. F. Stoddart, *Acc. Chem. Res.*, 2016, **49**, 262–273.
8. A. R. Pease, J. O. Jeppesen, J. F. Stoddart, Y. Luo, C. P. Collier and J. R. Heath, *Acc. Chem. Res.*, 2001, **34**, 433−444.
9. C. J. Bruns and J. F. Stoddart, *The Nature of the Mechanical Bond: From Molecules to Machines*, Wiley, New Jersey, 2016.
10. S. Erbas-Cakmak, D. A. Leigh, C. T. McTernan and A. L. Nussbaumer, *Chem. Rev.*, 2015, **115**, 10081−10206.
11. L. Zhang, V. Marcos and D. A. Leigh, *Proc. Natl. Acad. Sci. U. S. A.*, 2018, **115**, 9397–9404.
12. J. B. Reece, L. A. Urry, M. L. Cain, S. A. Wasserman, P. V. Minorsky, R. B. Jackson and N. A. Campbell, *Biology*, Pearson Education, Global ed of ninth edn., 2011.
13. Ó. Gutiérrez-Sanz, P. Natale, I. Márquez, M. C. Marques, S. Zacarias, M. Pita, I. A. C. Pereira, I. López-Montero, A. L. De Lacey and M. Vélez, *Angew. Chem. Int. Ed.*, 2016, **55**, 6216–6220.
14. M. Von Delius, E. M. Geertsema and D. A. Leigh, *Nat. Chem.*, 2010, **2**, 96–101.
15. C. Pezzato, M. T. Nguyen, C. Cheng, D. J. Kim, M. T. Otley and J. F. Stoddart, *Tetrahedron*, 2017, **73**, 4849−4857.
16. Y. Qiu, L. Zhang, C. Pezzato, Y. Feng, W. Li, M. T. Nguyen, C. Cheng, D. Shen, Q.-H. Guo, Y. Shi, K. Cai, F. M. Alsubaie, R. D. Astumian and J. F. Stoddart, *J. Am. Chem. Soc.*, 2019, **141**, 17472–17476.
17. R. D. Astumian, C. Pezzato, Y. Feng, Y. Qiu, P. R. McGonigal, C. Cheng and J. F. Stoddart, *Materials Chemistry Frontiers*, 2020, **4**, 1304–1314.
18. C. Cheng, P. R. McGonigal, W.-G. Liu, H. Li, N. A. Vermeulen, C. Ke, M. Frasconi, C. L. Stern, W. A. Goddard Iii and J. F. Stoddart, *J. Am. Chem. Soc.*, 2014, **136**, 14702−14705.
19. C. Cheng, T. Cheng, H. Xiao, M. D. Krzyaniak, Y. Wang, P. R. McGonigal, M. Frasconi, J. C. Barnes, A. C. Fahrenbach, M. R. Wasielewski, W. A. Goddard and J. F. Stoddart, *J. Am. Chem. Soc.*, 2016, **138**, 8288−8300.
20. T. Kudernac, N. Ruangsupapichat, M. Parschau, B. Maciá, N. Katsonis, S. R. Harutyunyan, K.-H. Ernst and B. L. Feringa, *Nature*, 2011, **479**, 208–211.

21. J. D. Badjic, C. M. Ronconi, J. F. Stoddart, V. Balzani, S. Silvi and A. Credi, *J. Am. Chem. Soc.*, 2006, **128**, 1489–1499.
22. D. A. Leigh, J. K. Y. Wong, F. Dehez and F. Zerbetto, *Nature*, 2003, **424**, 174–179.
23. S. Erbas-Cakmak, S. D. P. Fielden, U. Karaca, D. A. Leigh, C. T. McTernan, D. J. Tetlow and M. R. Wilson, *Science*, 2017, **358**, 340–343.
24. Q.-H. Guo, Y. Qiu, X. Kuang, J. Liang, Y. Feng, L. Zhang, Y. Jiao, D. Shen, R. D. Astumian and J. F. Stoddart, *J. Am. Chem. Soc.*, 2020, **142**, 14443−14449.
25. M. Jensen, R. Kristensen, S. S. Andersen, D. Bendixen and J. O. Jeppesen, *Chem. Eur. J.*, 2020, **26**, 6165−6175.
26. S. S. Andersen, A. W. Saad, R. Kristensen, T. S. Pedersen, L. J. O'Driscoll, A. H. Flood and J. O. Jeppesen, *Org. Biomol. Chem.*, 2019, **17**, 2432−2441.
27. S. S. Andersen, A. I. Share, B. L. C. Poulsen, M. Kørner, T. Duedal, C. R. Benson, S. W. Hansen, J. O. Jeppesen and A. H. Flood, *J. Am. Chem. Soc.*, 2014, **136**, 6373−6384.
28. J. W. Choi, A. H. Flood, D. W. Steuerman, S. Nygaard, A. B. Braunschweig, N. N. P. Moonen, B. W. Laursen, Y. Luo, E. DeIonno, A. J. Peters, J. O. Jeppesen, K. Xu, J. F. Stoddart and J. R. Heath, *Chem. Eur. J.*, 2006, **12**, 261−279.
29. J. O. Jeppesen, K. A. Nielsen, J. Perkins, S. A. Vignon, A. Di Fabio, R. Ballardini, M. T. Gandolfi, M. Venturi, V. Balzani, J. Becher and J. F. Stoddart, *Chem. Eur. J.*, 2003, **9**, 2982−3007.
30. C. R. Benson, C. Maffeo, E. M. Fatila, Y. Liu, E. G. Sheetz, A. Aksimentiev, A. Singharoy and A. H. Flood, *Proc. Natl. Acad. Sci. U. S. A.*, 2018, **115**, 9391−9396.
31. C. Pezzato, C. Cheng, J. F. Stoddart and R. D. Astumian, *Chem. Soc. Rev.*, 2017, **46**, 5491−5507.
32. J. W. Steed and J. L. Atwood, *Supramolecular Chemistry*, Wiley, Chippenham, Wiltshire, 2nd edn., 2009.
33. S. Nygaard, K. C. F. Leung, I. Aprahamian, T. Ikeda, S. Saha, B. W. Laursen, S.-Y. Kim, S. W. Hansen, P. C. Stein, A. H. Flood, J. F. Stoddart and J. O. Jeppesen, *J. Am. Chem. Soc.*, 2007, **129**, 960−970.
34. A. Coskun, M. Banaszak, R. D. Astumian, J. F. Stoddart and B. A. Grzybowski, *Chem. Soc. Rev.*, 2012, **41**, 19−30.
35. A. C. Fahrenbach, C. J. Bruns, H. Li, A. Trabolsi, A. Coskun and J. F. Stoddart, *Acc. Chem. Res.*, 2014, **47**, 482–493.
36. M. Xue, Y. Yang, X. Chi, X. Yan and F. Huang, *Chem Rev*, 2015, **115**, 7398–7501.
37. J. O. Jeppesen and J. Becher, *Eur. J. Org. Chem.*, 2003, 3245−3266.
38. D. Canevet, M. Sallé, G. Zhang, D. Zhang and D. Zhu, *Chem. Commun.*, 2009, 2245−2269.
39. H. V. Schröder and C. A. Schalley, *Beilstein J. Org. Chem.*, 2018, **14**, 2163−2185.
40. S. Nygaard, B. W. Laursen, A. H. Flood, C. N. Hansen, J. O. Jeppesen and J. F. Stoddart, *Chem. Commun.*, 2006, 144−146.
41. V. Serreli, C.-F. Lee, E. R. Kay and D. A. Leigh, *Nature*, 2007, **445**, 523–527.
42. A. Trabolsi, A. C. Fahrenbach, S. K. Dey, A. I. Share, D. C. Friedman, S. Basu, T. B. Gasa, N. M. Khashab, S. Saha, I. Aprahamian, H. A. Khatib, A. H. Flood and J. F. Stoddart, *Chem. Commun.*, 2010, **46**, 871−873.
43. K. D. Zhang, X. Zhao, G. T. Wang, Y. Liu, Y. Zhang, H. J. Lu, X. K. Jiang and Z. T. Li, *Angew. Chem. Int. Ed.*, 2011, **50**, 9866–9870.
44. T. Avellini, H. Li, A. Coskun, G. Barin, A. Trabolsi, A. N. Basuray, S. K. Dey, A. Credi, S. Silvi, J. F. Stoddart and M. Venturi, *Angew. Chem. Int. Ed.*, 2012, **51**, 1611−1615.
45. S. Di Motta, T. Avellini, S. Silvi, M. Venturi, X. Ma, H. Tian, A. Credi and F. Negri, *Chem. Eur. J.*, 2013, **19**, 3131–3138.
46. W.-K. Wang, Z.-Y. Xu, Y.-C. Zhang, H. Wang, D.-W. Zhang, Y. Liu and Z.-T. Li, *Chem. Commun.*, 2016, **52**, 7490–7493.
47. B. Brough, B. H. Northrop, J. J. Schmidt, H.-R. Tseng, K. N. Houk, J. F. Stoddart and C.-M. Ho, *Proc. Natl. Acad. Sci. U. S. A.*, 2006, **103**, 8583−8588.
48. F. M. Raymo and J. F. Stoddart, *Chem. Rev.*, 1999, **99**, 1643−1664.
49. S.-H. Chiu, S. J. Rowan, S. J. Cantrill, P. T. Glink, R. L. Garrell and J. F. Stoddart, *Org. Lett.*, 2000, **2**, 3631−3634.
50. A. Affeld, G. M. Hübner, C. Seel and C. A. Schalley, *Eur. J. Org. Chem.*, 2001, 2877−2890.
51. H.-L. Sun, H.-Y. Zhang, Z. Dai, X. Han and Y. Liu, *Chem. Asian J.*, 2017, **12**, 265−270.
52. J. O. Jeppesen, J. Perkins, J. Becher and J. F. Stoddart, *Angew. Chem. Int. Ed.*, 2001, **40**, 1216−1221.
53. A. Sørensen, S. S. Andersen, A. H. Flood and J. O. Jeppesen, *Chem. Commun.*, 2013, **49**, 5936−5938.
54. P. L. Anelli, P. R. Ashton, R. Ballardini, V. Balzani, M. Delgado, M. T. Gandolfi, T. T. Goodnow, A. E. Kaifer, D. Philp, M. Pietraszkiewicz, L. Prodi, M. V. Reddington, A. M. Z. Slawin, N. Spencer, J. F. Stoddart, C. Vicent and J. Williams David, *J. Am. Chem. Soc.*, 1992, **114**, 193−218.
55. J. O. Jeppesen, S. Nygaard, S. A. Vignon and J. F. Stoddart, *Eur. J. Org. Chem.*, 2005, 196−220.
56. S. S. Andersen, M. Jensen, A. Sørensen, E. Miyazaki, K. Takimiya, B. W. Laursen, A. H. Flood and J. O. Jeppesen, *Chem. Commun.*, 2012, **48**, 5157−5159.
57. R. Kristensen, S. S. Andersen, G. Olsen and J. O. Jeppesen, *J. Org. Chem.*, 2017, **82**, 1371−1379.
58. J. O. Jeppesen, S. A. Vignon and J. F. Stoddart, *Chem. Eur. J.*, 2003, **9**, 4611−4625.
59. S. Nygaard, C. N. Hansen and J. O. Jeppesen, *J. Org. Chem.*, 2007, **72**, 1617−1626.
60. N. Koumura, E. M. Geertsema, M. B. Van Gelder, A. Meetsma and B. L. Feringa, *J. Am. Chem. Soc.*, 2002, **124**, 5037−5051.
61. H. Li, C. Cheng, P. R. McGonigal, A. C. Fahrenbach, M. Frasconi, W.-G. Liu, Z. Zhu, Y. Zhao, C. Ke, J. Lei, R. M. Young, S. M. Dyar, D. T. Co, Y.-W. Yang, Y. Y. Botros, W. A. Goddard, M. R. Wasielewski, R. D. Astumian and J. F. Stoddart, *J. Am. Chem. Soc.*, 2013, **135**, 18609−18620.
62. M. Asakawa, W. Dehaen, G. L'Abbé, S. Menzer, J. Nouwen, F. M. Raymo, J. F. Stoddart and D. J. Williams, *J. Org. Chem.*, 1996, **61**, 9591−9595.
63. M. Döbbelin, I. Azcune, M. Bedu, A. Ruiz De Luzuriaga, A. Genua, V. Jovanovski, G. Cabañero and I. Odriozola, *Chem. Mater.*, 2012, **24**, 1583–1590.
64. H. E. Gottlieb, V. Kotlyar and A. Nudelman, *J. Org. Chem.*, 1997, **62**, 7512−7515.